Inorganic Chemistry

ARTICLE

pubs.acs.org/IC

^{11}B NMR Sensing of d-Block Metal Ions in Vitro and in Cells Based on the Carbon−Boron Bond Cleavage of Phenylboronic Acid-Pendant Cyclen (Cyclen = 1,4,7,10-Tetraazacyclododecane)

Masanori Kitamura,[†,‡] Toshihiro Suzuki,[§,‡] Ryo Abe,[§,‡] Takeru Ueno,[†] and Shin Aoki*[,†,‡]

[†]Faculty of Pharmaceutical Sciences, Tokyo University of Science, 2641 Yamazaki, Noda 278-8510, Japan

[‡]Center for Technologies against Cancer (CTC) and [§]Research Institute for Biological Sciences, Tokyo University of Science, 2669 Yamazaki, Noda 278-0022, Japan

Supporting Information

ABSTRACT: Noninvasive magnetic resonance imaging (MRI) including the "chemical shift imaging (CSI)" technique based on ^{1}H NMR signals is a powerful method for the in vivo imaging of intracellular molecules and for monitoring various biological events. However, it has the drawback of low resolution because of background signals from intrinsic water protons. On the other hand, it is assumed that the ^{11}B NMR signals which can be applied to a CSI technique have certain advantages, since boron is an ultratrace element in animal cells and tissues. In this manuscript, we report on the sensing of biologically indispensable d-block metal cations such as zinc, copper, iron, cobalt, manganese, and nickel based on ^{11}B NMR signals of simple phenylboronic acid-pendant cyclen (cyclen = 1,4,7,10-tetraazacyclododecane), L^6 and L^7, in aqueous solution at physiological pH. The results indicate that the carbon−boron bond of L^6 is cleaved upon the addition of Zn^{2+} and the broad ^{11}B NMR signal of L^6 at 31 ppm is shifted upfield to 19 ppm, which corresponds to the signal of $B(OH)_3$. ^{1}H NMR, X-ray single crystal structure analysis, and UV absorption spectra also provide support for the carbon−boron bond cleavage of ZnL^6. Because the cellular uptake of L^6 was very small, a more cell-membrane permeable ligand containing the boronic acid ester L^7 was synthesized and investigated for the sensing of d-block metal ions using ^{11}B NMR. Data on ^{11}B NMR sensing of Zn^{2+} in Jurkat T cells using L^7 is also presented.

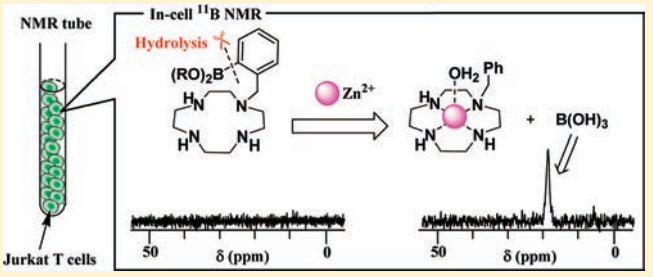

INTRODUCTION

d-Block metal cations such as zinc, copper, iron, cobalt, manganese, and nickel are involved in one-third of all human proteins as catalytic centers and structural cofactors, which makes them essential for life.[1] To maintain the homeostasis of metal ions both at the cellular and at whole organism levels, nature uses sophisticated metal complexes with DNA, proteins, and other biomelecules.[2,3] For example, several families of proteins that are integral transmembrane transporters, metalloregulatory sensor proteins, and diffusible cytoplasmic metallochaperone proteins deliver the metal ions to target molecules. In recent years, it has been recognized that a metal imbalance in cells and tissues causes a number of diseases such as taste disorders, Alzheimer's disease, Menkes and Wilson's diseases, amyotrophic lateral sclerosism, and cancer.[1c,4] For example, it is well established that Zn^{2+} levels is markedly decreased in prostate cancer and other cancer cells.[5] Accordingly, considerable efforts have been devoted to the development of fluorescent molecular sensors for the metal cations in living systems.[6−10] However, this sensing technique sometimes suffers from photobleaching of the fluorescent molecule and invisibility especially in tissue more than a few millimeters in depth because of light scattering and absorption. In addition, fluorescent sensors for cellular paramagnetic metal ions such as copper, iron, and nickel have remained underdeveloped[11] because these metals typically act as fluorescence quenchers.[12]

In this regard, ^{1}H magnetic resonance imaging (MRI) is a powerful method and is a widely used medical imaging technique for in vivo visualization because it is a noninvasive method capable of producing three-dimensional images of opaque organisms.[13] However, recent studies dealing with the MRI detection of metal ions[14] such as Zn^{2+},[15] Cu^{2+}/Cu^{+},[16] Fe^{2+},[17] and Ca^{2+}[18,19] are mostly limited to Gd^{3+}-based contrast agents that are used to observe changes in ^{1}H NMR signals. Furthermore, there are only a few reports that describe the MRI detection of metal cations in cells.[14a]

Meanwhile, it has been established that 1,4,7,10-tetraazacyclododecane (cyclen, L^1) forms extremely stable complexes with metal ions such as Zn^{2+}, Cu^{2+}, Ni^{2+}, Mn^{4+}/Mn^{3+}, and Co^{3+} in aqueous solutions at neutral pH (Scheme 1 depicted for Zn^{2+} complex **1** (ZnL^1))[20−24] and Zn^{2+}-selective cyclen-based fluorescent molecules (Chart 1) such as **2** (L^2),[8] **3** (L^3),[9] **4a** (L^4),[10a,b] and **4b** (L^5).[10c] It should be noted that Zn^{2+} in **1a** possesses

Received: July 15, 2011
Published: October 19, 2011

strong Lewis acidity which facilitates the deprotonation of Zn^{2+}-bound H_2O to form **1b** even at neutral pH (pK_a = 7.8).[10b,c] Moreover, the Zn^{2+}-bound HO^- in **1b** can also function as a nucleophile or base.

The objective of this work was to focus on the chemical and spectroscopic behaviors of simple Zn^{2+}−cyclen complexes containing a Lewis acidic boronic acid side chain such as **5** (L^6) and **6** (L^7) (Scheme 2). It is because the boron is regarded as a nonessential or "ultratrace" element in mammals[25] and the ^{11}B nucleus has higher NMR sensitivity (16.5% for ^{11}B and 2.0% for ^{10}B relative to ^1H NMR) and higher natural abundance than ^{10}B (80.4% for ^{11}B vs 19.6% for ^{10}B),[26] while both isotopes have almost similar structures and binding or pharmacokinetic effects of the agents. We were interested in structural changes of the sp^2 boron in metal-free **5** and **6** to the sp^3 boron in the corresponding metal complexes **7** and **8** at neutral pH, based on the hypothesis that the metal-bound H_2O (or HO^-) would interact with boron, resulting in a ^{11}B NMR spectral change.

In this manuscript, we report on our finding about the C−B bond hydrolysis of **5** and **6** upon the formation of complexes with Zn^{2+} and other d-block metal ions to give **9** (ML^8) and boric acid ($B(OH)_3$), resulting in a substantial and measurable change in the ^{11}B NMR signals (Scheme 2). Data on the in-cell ^{11}B NMR for the sensing of Zn^{2+} in Jurkat T cells using **6** are also presented. These data present a basic concept for sensing of Zn^{2+} and other d-block metal ions based on shifts in the ^{11}B NMR signal, the mechanism of which is different from that of Gd^{3+}-based contrast agents.

Scheme 1

Chart 1

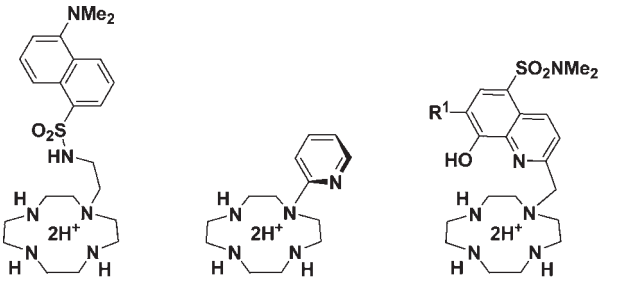

EXPERIMENTAL SECTION

General Information. $ZnSO_4 \cdot 7H_2O$ and $CuSO_4 \cdot 5H_2O$ were purchased from Yoneyama Chemical Industry Co. Ltd. $Zn(NO_3)_2 \cdot 6H_2O$, $MgCl_2 \cdot 6H_2O$, $Cd(NO_3)_2 \cdot 4H_2O$, and $FeCl_3 \cdot 6H_2O$ were obtained from Kanto Chemical Co. Ltd. $FeCl_2 \cdot 4H_2O$, $NiCl_2$, and $CoCl_2$ were purchased from Wako Pure Chemical Industries, Ltd. Anhydrous $CaCl_2$ was obtained from Nacalai Tesque, Inc. $MnSO_4 \cdot H_2O$ was purchased from Sigma-Aldrich Co. Acetonitrile (CH_3CN) and dichloromethane (CH_2Cl_2) were distilled from calcium hydride. All aqueous solutions were prepared using deionized and distilled water. The Good's buffer reagents (Dojindo) were obtained from commercial sources: MES (2-morpholinoethanesulfonic acid, pK_a = 4.8), HEPES (*N*-(2-hydroxyethyl)piperazine-*N*′-2-ethanesulfonic acid, pK_a = 7.5), EPPS (*N*-(2-hydroxyethyl)piperazine-*N*′-3-propanesulfonic acid, pK_a = 8.0), CHES (2-(cyclohexylamino)ethanesulfonic acid, pK_a = 9.5), CAPS (3-(cyclohexylamino)propanesulfonic acid, pK_a = 10.4). Buffer solutions (acetic acid/sodium acetate, pH 4; MES, pH 5, 5.5, 6; HEPES, pH 7, 7.4; EPPS, pH 8, 8.5; CHES, pH 9; CAPS, pH 10, 11) were used. All other reagents and solvents were of the highest commercial quality and were used without further purification unless otherwise noted. Melting points were measured on a YANACO Micro Melting Point Apparatus and are uncorrected. IR spectra were recorded on a JASCO

Scheme 2

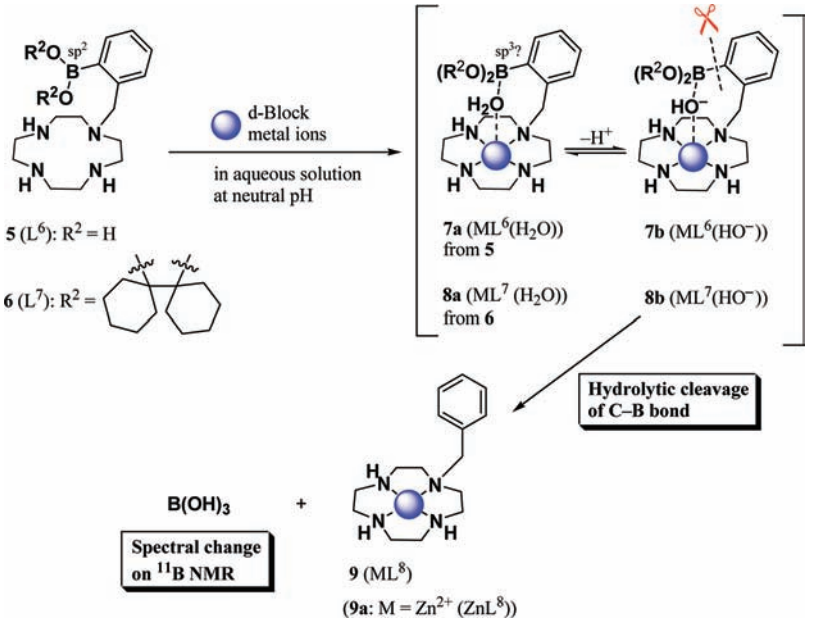

dx.doi.org/10.1021/ic201507q |*Inorg. Chem.* 2011, 50, 11568–11580

FTIR-410 and a PerkinElmer Spectrum100 spectrophotometer at room temperature (rt). ^{1}H (400 MHz), ^{13}C (100 MHz), and ^{11}B (128 MHz) NMR spectra were recorded on a JEOL Lambda 400 spectrometer. ^{1}H (300 MHz) and ^{13}C (75 MHz) NMR spectra were recorded on a JEOL Always 300 spectrometer. Chemical shifts (δ) in $CDCl_3$ were determined relative to an internal reference of tetaramethylsilane (TMS) for ^{1}H NMR and $CDCl_3$ for ^{13}C NMR. The sodium salt of 3-(trimethylsilyl)propionic-2,2,3,3-d_4 acid (TSP) was used as an external reference for ^{1}H NMR and 1,4-dioxane for ^{13}C NMR measurements in D_2O. ^{11}B NMR spectra were measured in a quartz NMR tube using boron trifluoride diethyl ether complex in $CDCl_3$ as an external reference (0 ppm). The pD values in D_2O were corrected for a deuterium isotope effect using pD = (pH-meter reading) + 0.40. Elemental analyses were performed on a Perkin-Elmer CHN 2400 analyzer. Electrospray ionization (ESI) mass spectra were recorded on a JEOL JMS-SX102A and Varian 910-MS. Inductively coupled plasma−atomic emission spectrometry (ICP−AES) measurements were performed on a Shimadzu ICPE-9000. Thin-layer chromatography (TLC) was performed using a Merck Silica 5554 (silica gel) TLC plate. Silica gel column chromatographies were performed using Fuji Silysia Chemical FL-100D or Fuji Silysia Chromatorex Chromatography Silica Gel NH.

1-[(2-Boronophenyl)methyl]-4,7,10-tris(*tert*-butyloxycarbonyl)-1,4,7,10-tetraazacyclododecane (12). A mixture of 3Boc-cyclen **10**[27] (1.18 g, 2.50 mmol), 2-(bromomethyl)phenylborane **11**[28] (806 mg, 3.75 mmol), and K_2CO_3 (691 mg, 5.00 mmol) in CH_3CN (10 mL) was refluxed for 3 h. After the addition of water, the reaction mixture was extracted with CH_2Cl_2. The combined extract was washed with brine, dried over Na_2SO_4, and evaporated. The resulting residue was purified by silica gel column chromatography (hexane/AcOEt = 1:1 to MeOH:CH_2Cl_2 = 1:10) to afford **12** as a colorless amorphous solid (1.31 g, 86% yield): mp 74−77 °C. ^{1}H NMR (400 MHz, $CDCl_3$ with 3 drops of MeOH-d_4/TMS) δ = 1.43−1.50 (27H, m), 2.83 (4H, brs), 3.35 (4H, brs), 3.44 (4H, brs), 3.52 (4H, brs), 3.77 (2H, brs), 7.16 (1H, brs), 7.29−7.33 (2H, m), 7.83 (1H, brs) ppm; ^{13}C NMR (100 MHz, $CDCl_3$ with 3 drops of MeOH-d_4) δ = 28.21, 28.24, 28.30, 28.31, 45.95 (br), 48.48 (br), 49.83 (br), 60.95, 80.14, 80.19, 127.23, 129.72, 130.35, 135.07, 135.93, 140.69, 156.21 ppm; ^{11}B NMR (128 MHz, $CDCl_3$ with 3 drops of MeOH-d_4): δ = 29.02 (brs) ppm; IR (neat): ν = 3390, 2976, 2930, 1694, 1463, 1415, 1366, 1250, 1165, 1031, 921, 858, 732, 647, 438 cm^{-1}. Anal. Calcd (%) for $C_{30}H_{51}BN_4O_8$: C, 59.40; H, 8.47; N, 9.24. Found: C, 59.11; H, 8.66; N, 8.84. HRMS (ESI$^+$): calcd for [M ($C_{30}H_{51}{}^{10}BN_4O_8$) + H]$^+$, 606.3897: found, 606.3909.

1-[(2-Boronophenyl)methyl]-1,4,7,10-tetraazacyclododecane Trifluoroacetic Acid Salt (5·2TFA). To a CH_2Cl_2 solution (2 mL) of **12** (1.18 g, 2.50 mmol) was added trifluoroacetic acid (2 mL) at rt, and the reaction mixture was stirred for 1 h. After evaporation, the resulting residue was recrystallized from Et_2O/MeOH to give colorless crystals of **5** (476 mg, 89% yield), which were determined to be the 2TFA salt by elemental analysis and potentiometric pH titration. The obtained crystals were suitable for an X-ray crystal structure analysis: mp 163−166 °C (dec.). ^{1}H NMR (400 MHz, D_2O/TSP): δ = 2.88 (4H, brs), 3.02 (4H, brs), 3.14 (4H, t, J = 5.2 Hz), 3.18 (4H, t, J = 4.9 Hz), 3.89 (2H, s), 7.38 (1H, d, J = 7.6 Hz), 7.42−7.51 (2H, m), 7.64 (1H, d, J = 7.6 Hz) ppm; ^{13}C NMR (100 MHz, D_2O/1,4-dioxane): δ = 41.66, 41.75, 43.90, 48.78, 59.31, 116.37 (q, J_{C-F} = 291.7 Hz), 127.88, 130.04, 131.25, 133.43, 139.19, 162.87 (q, J_{C-F} = 35.3 Hz) ppm; ^{11}B NMR (128 MHz, $D_2O/BF_3\cdot Et_2O$): δ = 30.76 (brs) ppm; IR (KBr): ν = 3060, 2848, 1667, 1619, 1467, 1444, 1394, 1353, 1276, 1192, 1133, 1035, 1014, 937, 833, 796, 763, 739, 722, 659, 600, 505, 421 cm^{-1}. Anal. Calcd (%) for $C_{19}H_{29}BF_6N_4O_6$: C, 42.71; H, 5.47; N, 10.49. Found: C, 42.58; H, 5.29; N, 10.35. HRMS (ESI$^+$): calcd for [M ($C_{15}H_{27}{}^{10}BN_4O_2$) + H]$^+$, 306.2339: found, 306.2336.

Boronic Acid Ester (6). A EtOH solution (3 mL) of **5**·2TFA (162 mg, 0.3 mmol) and bicyclohexyl-1,1′-diol **13**[29] (59 mg, 0.3 mmol) was refluxed overnight. After concentration under reduced pressure, the residue was purified by column chromatography using Fuji Silysia Chromatorex Chromatography Silica Gel NH ($CHCl_3$/MeOH = 9:1) to afford the **6** as a colorless solid (133 mg, 95% yield): ^{1}H NMR (300 MHz, $CDCl_3$/TMS): δ = 1.15−1.33 (6H, m), 1.67−1.82 (14H, m), 2.54−2.67 (15H, m), 2.80 (4H, t, J = 4.9 Hz), 3.96 (2H, s), 7.21 (1H, td, J = 7.4, 1.0 Hz), 7.43 (1H, td, J = 7.5, 1.4 Hz), 7.58 (1H, d, J = 7.3 Hz), 7.81 (1H, dd, J = 7.4, 1.4 Hz) ppm; ^{13}C NMR (75 MHz, $CDCl_3$): δ = 22.33, 25.62, 32.26, 45.15, 46.27, 47.10, 51.57, 57.14, 84.41, 125.68, 128.12, 128.85, 130.86, 135.69, 146.11 ppm; ^{11}B NMR (128 MHz, $D_2O/BF_3\cdot Et_2O$): δ = 30.98 (brs) ppm; IR (ATR): ν = 2931, 2852, 1600, 1570, 1442, 1387, 1368, 1344, 1311, 1285, 1273, 1254, 1237, 1146, 1133, 1113, 1070, 1055, 1040, 937, 911, 826, 805, 748, 727, 671, 656, 545, 507 cm^{-1}. Anal. Calcd (%) for $C_{27}H_{45}BN_4O_2\cdot 0.5H_2O$: C, 67.92; H, 9.71; N, 11.73. Found: C, 68.03; H, 9.71; N, 11.47. HRMS (ESI$^+$): calcd for [M ($C_{27}H_{45}{}^{10}BN_4O_2$) + H]$^+$, 468.3749: found, 468.3745.

1-[(3-Boronophenyl)methyl]-4,7,10-tris(*tert*-butyloxycarbonyl)-1,4,7,10-tetraazacyclododecane (15). A mixture of 3Boc-cyclen **10**[27] (172 mg, 0.363 mmol), 3-(bromomethyl)phenylborane **14**[30] (78 mg, 0.363 mmol), and Na_2CO_3 (77 mg, 0.73 mmol) in CH_3CN (16 mL) was refluxed for 22 h. After filtration through a Celite pad, the filtrate was evaporated and purified by silica gel column chromatography (hexane/AcOEt = 3:2) to afford **15** as a colorless amorphous solid (192 mg, 87% yield): mp 118−121 °C. ^{1}H NMR (300 MHz, MeOH-d_4/TMS) δ = 1.43 (18H, brs), 1.49 (9H, s), 2.64 (4H, brs), 3.25−3.75 (14H, m), 7.25−7.31 (2H, m), 7.46−7.72 (2H, m) ppm; ^{13}C NMR (75 MHz, MeOH-d_4) δ = 28.86, 29.09, 48.23, 48.50, 50.76 (br), 56.56 (br), 57.91 (br), 80.73, 128.38, 132.70, 133.29, 133.91, 134.59, 136.70, 137.05, 137.43, 157.00, 157.18, 157.39 ppm; ^{11}B NMR (128 MHz, $D_2O/BF_3\cdot Et_2O$): δ = 29.02 (brs) ppm; IR (ATR): ν = 3377, 2977, 2934, 1684, 1459, 1415, 1364, 1323, 1270, 1249, 1151, 1108, 1048, 980, 859, 802, 772, 711, 673, 614, 555, 511 cm^{-1}. Anal. Calcd (%) for $C_{30}H_{51}BN_4O_8$: C, 59.40; H, 8.47; N, 9.24. Found: C, 59.24; H, 8.85; N, 8.99. HRMS (ESI$^+$): calcd for [M ($C_{30}H_{51}{}^{10}BN_4O_8$) + Na]$^+$, 628.3735: found, 628.3729.

1-[(3-Boronophenyl)methyl]-1,4,7,10-tetraazacyclododecane (16). To a solution of **15** (289 mg, 0.477 mmol) in CH_2Cl_2 (3 mL) was added trifluoroacetic acid (2 mL) at rt, and the reaction mixture was allowed to stir overnight. After evaporation, the resulting residue was purified by column chromatography using Fuji Silysia Chromatorex Chromatography Silica Gel NH ($CHCl_3$/MeOH = 9:1) to afford the **16** as a colorless amorphous solid (133 mg, 87% yield): mp 101−105 °C. ^{1}H NMR (400 MHz, D_2O (pD 9.2)/TSP): δ = 2.90−2.98 (8H, m), 3.05−3.08 (4H, m), 3.11−3.15 (4H, m), 3.80 (2H, s), 7.26 (1H, d, J = 7.2 Hz), 7.38 (1H, t, J = 7.2 Hz), 7.57 (1H, s), 7.61 (1H, d, J = 7.2 Hz) ppm; ^{13}C NMR (100 MHz, D_2O (pD 9.2)/1,4-dioxane): δ = 41.81−42.22 (m), 43.95−44.33 (m), 48.34−48.64 (m), 57.20−57.69 (m), 66.73−67.66 (m), 128.04−128.21 (m), 128.77−128.99 (m), 131.94, 133.30, 133.41, 134.52 ppm; ^{11}B NMR (128 MHz, D_2O (pD 9.2)/$BF_3\cdot Et_2O$): δ = 12.45 (brs) ppm; IR (ATR): ν = 3278, 2823, 1648, 1600, 1581, 1447, 1377, 1352, 1291, 1256, 1198, 1146, 1112, 1080, 1043, 1016, 979, 944, 796, 746, 719, 660, 626, 581, 534, 499 cm^{-1}. Anal. Calcd (%) for $C_{15}H_{27}BN_4O_2\cdot$MeOH: C, 56.81; H, 9.24; N, 16.56. Found: C, 56.80; H, 9.09; N, 16.20. HRMS (ESI$^+$): calcd for [M ($C_{15}H_{27}{}^{10}BN_4O_2$) + H]$^+$, 306.2340: found, 306.2336.

Crystallographic Study of 5·2TFA (L^6). Crystals of **5**·2TFA were obtained from Et_2O/MeOH at rt. All measurements were made on a Rigaku Saturn CCD area detector with graphite monochromated Mo−Kα radiation at 123 K. $C_{19}H_{29}B_1F_6N_4O_6$, M_r = 534.26, a colorless platelet crystal, crystal size 0.40 × 0.35 × 0.20 mm, monoclinic, space group $P2_1/c$ (#14), a = 9.392(5), b = 12.179(7), c = 21.872(12) Å,

β = 94.892(3)°, V = 2493(2) Å^3, Z = 4, D_{calc} = 1.423 g·cm^{-3}, 17564 measured reflections, 5601 unique reflections, $2\theta_{max}$ = 55.0°, $R1$ (w$R2$) = 0.0754 (0.2009), GOF = 1.160. Details of the crystallographic analysis of **5**·2TFA are given in the Supporting Information, Tables S2−S4 and CIF.

Complexation of 5 (L^6) with Zn^{2+} and Crystallographic Study of the Complex 9a (ZnL^8). A solution of $Zn(NO_3)_2 \cdot 6H_2O$ (44 mg, 0.15 mmol) in water (0.5 mL) was added to an aqueous solution (1 mL) of **5** (80 mg, 0.15 mmol) at rt, and pH of the reaction mixture was adjusted to 7 by adding 0.1 M $NaOH_{aq}$. After evaporation, the resulting residue was recrystallized from water (0.2 mL) to provide colorless crystals (36 mg, 40% yield). The ^{1}H NMR spectrum of the obtained crystals was consistent with that of an authentic sample of **9a**.[31] The obtained crystals were suitable for an X-ray crystal structure analysis and determined as the complex **9a** and boric acid ($B(OH)_3$). All measurements were made on a Rigaku Saturn CCD area detector with graphite monochromated Mo−Kα radiation at 123 K. $C_{38}H_{55}B_1F_{12}N_8O_{13}$, M_r = 1201.45, a colorless block crystal, crystal size 0.30 × 0.25 × 0.20 mm, triclinic, space group $P\bar{1}$ (#2), a = 9.968(6), b = 16.226(8), c = 16.718(9) Å, α = 71.955(18)°, β = 89.71(2)°, γ = 77.420(19)°, V = 2504(2) Å^3, Z = 2, D_{calc} = 1.594 g·cm^{-3}, 16602 measured reflections, 8975 unique reflections, $2\theta_{max}$ = 51.0°, $R1$ (w$R2$) = 0.0456 (0.1251), GOF = 0.999. Full details of crystallographic analysis are given in the Supporting Information, Table S5−S7 and CIF.

Potentiometric pH Titrations. The preparation of the test solutions and the method used for calibration of the electrode system (Potentiometric Automatic Titrator AT-400 and Auto Piston Buret APB-410, Kyoto Electronics Manufacturing, Co. Ltd.) with a Kyoto Electronics Manufacturing Co. Combination pH Electrode 98100C171 have been described previously.[10,27] All of the test solutions (50 mL) were maintained under an argon (>99.999% purity) atmosphere. The potentiometric pH titrations were performed with I = 0.1 ($NaNO_3$) at 25.0 ± 0.1 °C (0.1 M aqueous NaOH was used as the base). The deprotonation constants were determined using the "BEST" software program.[32] The K_W (equivalent to $a_{H+}a_{OH-}$), K_W (equivalent to $[H^+][HO^-]$), and f_{H+} values used at 25 °C were $10^{-14.00}$, $10^{-13.79}$, and 0.825, respectively. The corresponding mixed constants K_2 (= [HO^--bound species]a_{H+}/[H_2O-bound species]), were derived using $[H^+] = a_{H+}/f_{H+}$. The percentage species distribution values against pH (= −log[H^+] + 0.084) were obtained using the "SPE" software program.[32]

General Procedure for Detection of d-Block Metal Ions by ^{11}B NMR Spectroscopy. A solution (0.6 mL) of boronic acid **5** (L^6) or boronic acid ester **6** (L^7) ([**5**] = [**6**] = 20 mM) prepared in HEPES buffer (1 M, pD 7.4) was placed into a quartz NMR tube. After measuring the ^{11}B NMR spectrum of the ligand alone, an equimolar amount of the given metal ions in D_2O was added, and ^{11}B NMR spectra were collected with a sweep width of 38022 Hz, 4096 data points, a 45° pulse width, a 0.16 s recycle time, and 2850 scans. Each spectrum was processed with 4.6 Hz line broadening and referenced to external $BF_3 \cdot Et_2O$ in $CDCl_3$ as δ = 0 ppm (Figure 5 and Table 2).

Typical Procedure for the Uptake of 5 (L^6) and 6 (L^7) in Jurkat T Cells and Its Quantitative Analysis by ICP−AES. A culture medium of 10% fetal calf serum−Roswell Park Memorial Institute (FCS−RPMI) medium with **5** or **6** (final concentration 33 μM) was prepared using a stock solution of **5** (100 mM) in water or **6** (10 mM) in dimethylsulfoxide (DMSO). For **5**, DMSO was added to adjust the concentration of DMSO in the medium ([DMSO] = 0.33% v/v). 10% FCS−RPMI including DMSO (0.33% v/v in the medium) was also prepared for use as a negative control. Jurkat T cells (2 × 10^7 cells) were incubated with the medium (20 mL) containing either **5**, **6**, or DMSO (negative control) at 37 °C in a 5% CO_2 environment. After a 1 h period of incubation, the cells were collected by centrifugation (1400 rpm ×7 min at 4 °C) and washed with 0.5% calf serum−Roswell Park Memorial Institute (CS−RPMI) medium and PBS (phosphate buffered saline) to remove extracellular **5**, **6**, or DMSO. The cells were collected again by centrifugation (2000 rpm ×10 min at 4 °C) and then lysed in RIPA (Radio-Immunoprecipitation Assay) buffer (500 μL) on ice for 30 min. After centrifugation (15000 rpm ×10 min at 4 °C), the resulting supernatant liquids (400 μL) were diluted with 1 N HCl (5 mL) and water (4.6 mL) to give sample solutions (10 mL). These sample solutions were prepared in triplicate. The amount of boron in the sample solutions (Figure 8) was quantitatively determined by ICP−AES (Shimadzu ICPE-9000, emission at 249.773 nm) using a standardized curve of $B(OH)_3$.

Typical Procedure of in-Cell ^{11}B NMR Using 6 for the Detection of Zn^{2+} in Jurkat T Cells. Jurkat T cells (4 × 10^8 cells) were incubated in 10% FCS−RPMI medium (400 mL) of **6** (final concentration 33 μM) at 37 °C in a 5% CO_2 environment for 1 h. After collecting the cells by centrifugation (1400 rpm ×7 min at 4 °C) and washing with 0.5% CS−RPMI to remove extracellular **6**, either Zn^{2+}−pyrithione[33] (2.5 or 10 μM in the culture medium) or DMSO (negative control) in 10% FCS−RPMI was added and incubated for 20 min in a 5% CO_2 environment. All of the cells were collected by centrifugation (1400 rpm ×7 min at 4 °C) and washed with 0.5% CS−RPMI and then PBS buffer (prepared in D_2O). The cell pellets obtained by these centrifugations (1400 rpm ×7 min at 4 °C) were placed in quartz NMR tubes using 200 μL PBS buffer (in D_2O), and ^{11}B NMR spectra of the cell pellets were measured using 830000 scans and the same parameters as described above. Each spectrum was processed with 4.6 Hz line broadening and baseline correction, and referenced to external $BF_3 \cdot Et_2O$ in $CDCl_3$ (as δ = 0 ppm).

RESULTS AND DISCUSSION

Synthesis of 5 (L^6), 6 (L^7), 16 (L^9), and X-ray Single Crystal Structure Analysis of 5 (L^6). We first synthesized **5** (L^6) and **6** (L^7) as outlined in Scheme 3. The reaction of Boc-protected cyclen (**10**[27]) with bromide (**11**[28]) afforded **12**, whose three Boc groups were deprotected by treatment with trifluoroacetic acid (TFA) to give **5** as the 2TFA salt (L^6·2TFA). The reaction of **5** with bicyclohexyl-1,1′-diol **13**[29] gave **6** (L^7). For comparison, the isomeric ligand **16** (L^9) was prepared in a similar manner as for **5** via **15**, which was synthesized from Boc-protected cyclen (**10**) and bromide **14**[30] (Scheme 3).

A single-crystal X-ray structure analysis of **5**·2TFA obtained from Et_2O/MeOH shows the presence of a carbon−boron bond and hydrogen bonding between hydroxyl groups of the boronic acid and the carboxylate group of the TFA^- O(1)−O(4) = 2.74 Å and O(2)−C(3) = 2.67 Å in Figure 1 (See also the structure **5**·2TFA in Scheme 3).

Deprotonation Constants of 5 (L^6) Determined by Potentiometric pH Titration. A typical potentiometric pH titration curve for 1.0 mM **5**·2TFA (L^6·2TFA) + 2.0 mM HNO_3 against aqueous 0.1 M NaOH with I = 0.1 ($NaNO_3$) at 25 °C (Figure 2) was analyzed for acid−base equilibrium (1−3). The deprotonation constants pK_{ai} (i = 1−5) of **5** were determined to be <3 (pK_{a1} and pK_{a2}), 8.4 ± 0.1 (pK_{a3}), 10.5 ± 0.1 (pK_{a4}), and >12 (pK_{a5}) using the "BEST" software program[32] (Table 1). For comparison, the pK_a values for cyclen, phenylboronic acid (**17**[34] in Chart 2), 2-(dimethylaminomethyl)phenylboronic acid (**18**[35] in Chart 2), and meta isomer **16** (L^9) are also listed in the Table 1.

For the assignment of the pK_a value of the $B(OH)_2$ portions of **5** (L^6) and **16** (L^9), ^{11}B NMR spectra were measured at pH 3−13. As shown in Figure 3, the pK_a values of the $B(OH)_2$

Scheme 3

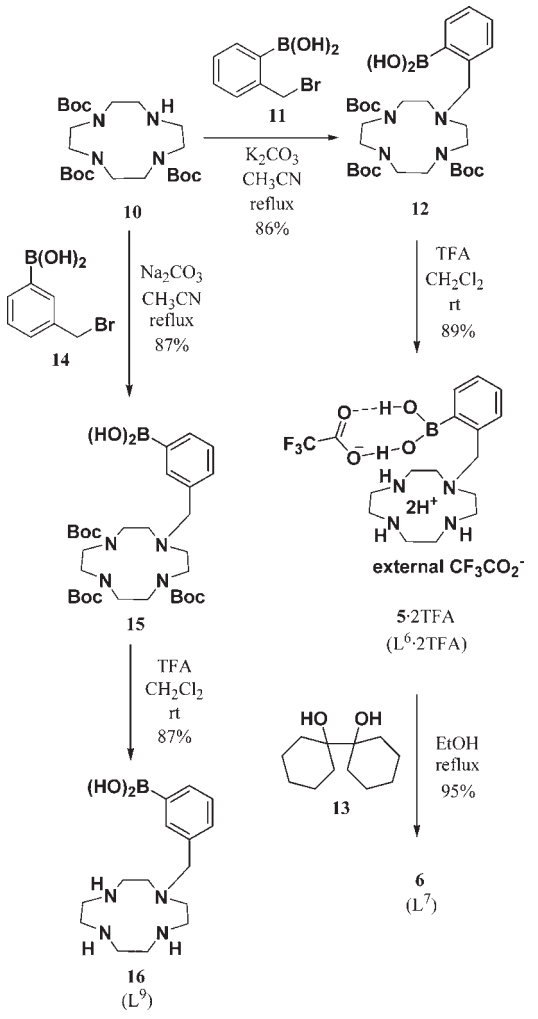

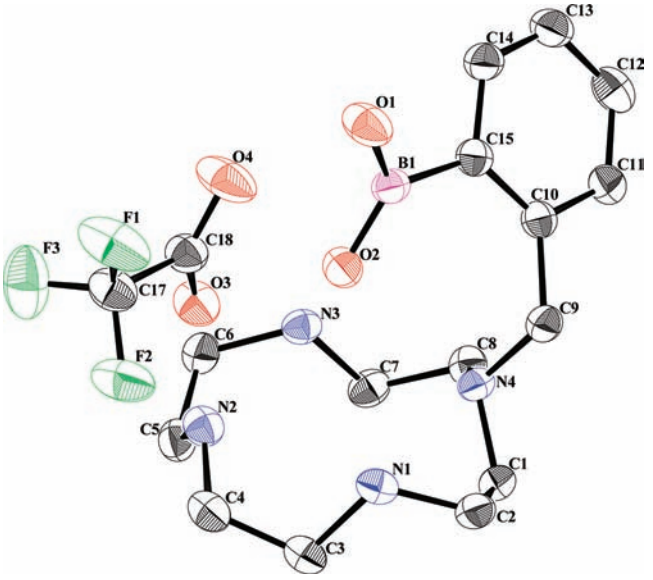

Figure 1. ORTEP drawing of **5**·2TFA salt (50% probability ellipsoids). Selected bond lengths [Å]: C(15)−B(1) 1.579(4), B(1)−O(1) 1.362(4), B(1)−O(2) 1.364(4), O(1)−O(4) 2.738, O(2)−O(3) 2.670. One external trifluoroacetate anion and hydrogen atoms have been omitted for clarity.

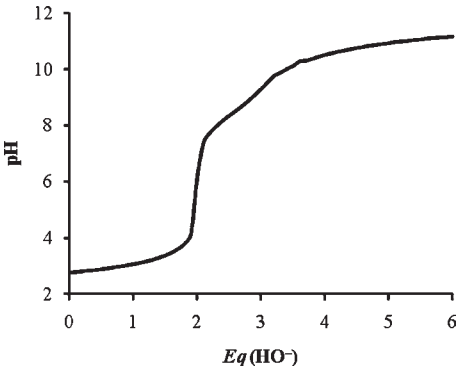

Figure 2. Typical potentiometric pH titration curve for 1.0 mM **5**·2TFA (L^6·2TFA) + 2.0 mM HNO_3 with I = 0.1 ($NaNO_3$) at 25 °C. *Eq* (HO^-) is the number of equivalents of base (NaOH) added.

Table 1. Deprotonation Constants (pK_{ai}) of Cyclen (L^1), Phenylboronic acid (17), 18, 5 (L^6), and 16 (L^9) in Aqueous Solution

	cyclen (L^1)[a]	**17**[b]	**18**[c]	**5** (L^6)[d]	**16** (L^9)[d]
pK_{a1}	<2	8.9	5.2	<3	<3
pK_{a2}	<2		11.8	<3	3.2
pK_{a3}	9.9			8.4	8.2
pK_{a4}	11.0			10.5	10.0
pK_{a5}				>12	>12

[a] From ref 10c. [b] From ref 34. [c] From ref 35. [d] The pK_a values determined by potentiometric pH titration with I = 0.1 ($NaNO_3$) at 25 °C.

portion of **5** and **16** are about 8.5−9, which are in fairly good agreement with the pK_{a3} values determined by potentiometric pH titration. It has been reported that the pK_a value of **17** is 8.9, and ^{11}B NMR signals of sp^2 and sp^3 boron appear at 25−35 ppm and 5−15 ppm, respectively.[36−38] Accordingly, we assigned the pK_{a3} of 8.4 and 8.2 to the $B(OH)_2$ parts of **5** and **16** and that the pK_{a1}, pK_{a2}, pK_{a4}, and pK_{a5} values of **5** and **16** correspond to the pK_a values of four nitrogens of the cyclen ring, as summarized in Scheme 4 and Scheme S1 in the Supporting Information (pK_{a1} and pK_{a2} are for **5**·4H$^+$ (H_4L^6) ⇄ **5**·3H$^+$ (H_3L^6) ⇄ **5**·2H$^+$ (H_2L^6), pK_{a4} for **19** ⇄ **20**, and pK_{a5} for **20** ⇄ **21** in Scheme 4).

Careful experiments revealed that a small shoulder appears at pD 9−12 in the pH-dependent ^{11}B NMR of **5** (Figure 3). In addition, the pK_{a4} value (10.5) is somehow greater than that of the regioisomer **16** (10.0). These data allowed us to consider some interactions between the cyclen ring and the $B(OH)_2$ portion in **5**. In general, the pK_a value of an ammonium ion is 9−10, but the pK_{a1} value from the ammonium portion of **18**·H$^+$ is reported to be 5.2, which is much smaller than that of typical ammonium cations.[35] On the other hand, the pK_{a2} value of **18** was determined to be 11.8, which is greater than that of **17** (8.9). Anslyn et al. explained these phenomena as displayed in Scheme 5.[36] Namely, the assumption is that there is an equilibrium between **18** and the (**18**·H$^+$·HO$^-$) form (middle in Scheme 5), in which an N−B dative bond interaction and an

dx.doi.org/10.1021/ic201507q |*Inorg. Chem.* 2011, 50, 11568–11580

Chart 2

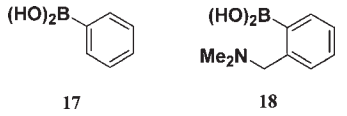

17 18

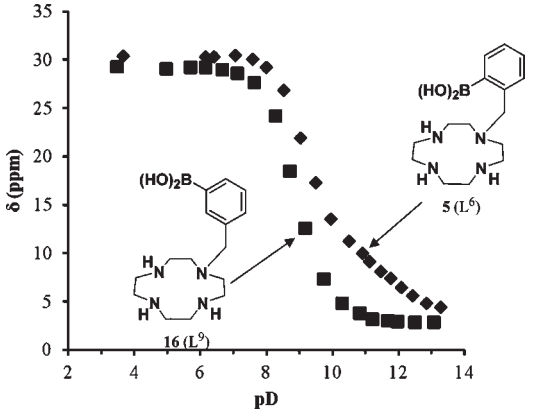

Figure 3. ^{11}B NMR spectral change of **5** (L^6) and **16** (L^9) with increasing pD at 25 °C and I = 0.5 ($NaNO_3$). [**5**] = [**16**] = 10 mM.

$N^+H\cdots HO{-}B^-$ interaction occur. From these data, we assume that some weak interactions occur between the nitrogen of the cyclen ring and the $B(OH)_2$ group of **5**, as displayed in **19a** and/or **19b** (Scheme 4).

$$(H_{(5-i)}L^6)^{(5-i)+} \rightleftarrows (H_{(4-i)}L^6)^{(4-i)+} + H^+ :$$

$$K_{ai}(L^6) = [(H_{(4-i)}L^6)^{(4-i)+}]\cdot a_{H+}/[(H_{(5-i)}L^6)^{(5-i)+}] \quad (i = 1,2) \tag{1}$$

$$(H_2L^6)^{2+} + H_2O \rightleftarrows (H_2L^6\cdot HO^-)^+ + H^+ :$$

$$K_{a3}(L^6) = [(H_2L^6\cdot HO^-)^+]\cdot a_{H+}/[(H_2L^6)^{2+}] \tag{2}$$

$$(H_{(6-i)}L^6\cdot HO^-)^{(5-i)+} \rightleftarrows (H_{(5-i)}L^6\cdot HO^-)^{(i-4)-} + H^+ :$$

$$K_{ai}(L^6) = [(H_{(5-i)}L^6\cdot HO^-)^{(i-4)-}]\cdot a_{H+}/[(H_{(6-i)}L^6\cdot HO^-)^{(5-i)+}] \quad (i = 4,5) \tag{3}$$

Detection of the C−B Bond Cleavage Reaction of 5 (L^6) upon Complexation with Zn^{2+}, As Evidenced by an X-ray Crystal Structure Analysis and ^{1}H NMR Spectra. Fine colorless crystals appeared after incubating a mixture of **5** (L^6) and Zn^{2+} in water at neutral pH and rt. Surprisingly, a single-crystal X-ray structure analysis showed no carbon−boron bond in the Zn^{2+} complex structure, and boric acid ($B(OH)_3$) was found as an external molecule in the crystal (Figure 4). This finding suggests that a carbon−boron bond is cleaved upon the complexation with Zn^{2+} to yield **9a** (Scheme 2). In addition, the ^{1}H NMR

Scheme 4

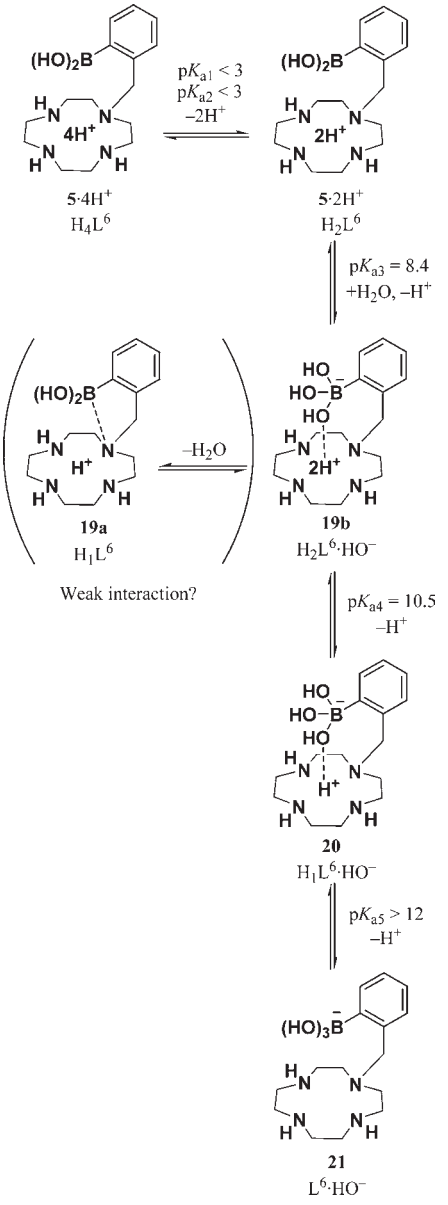

spectrum of the obtained complex was consistent with that of an authentic sample of **9a**[31] (data not shown), supporting the aforementioned phenomena.

^{11}B NMR Spectral Change of 5 (L^6) upon Complexation with Zn^{2+} and d-Block Metal Ions. The results of the X-ray crystal structure analysis and ^{1}H NMR of **9a** (ZnL^8) prompted us to measure the ^{11}B NMR spectral change of **5** upon complexation with Zn^{2+}. Figure 5a displays a ^{11}B NMR signal of **5** (20 mM) in the absence of Zn^{2+} in D_2O at pD 7.4 (1 M HEPES buffer) and 25 °C, and Figure 5b−f were collected after the addition of Zn^{2+} (20 mM) for 8 min of each measurement time. Upon the addition of Zn^{2+}, the broad signal of **5** at 31.1 ppm was shifted to 19.4 ppm, which coincides with the signal for $B(OH)_3$ (Figure 5g).[39] This carbon−boron cleavage reaction did not take place in the presence of Zn^{2+} at pD > 12 (Supporting Information, Figure S1).

dx.doi.org/10.1021/ic201507q |*Inorg. Chem.* 2011, 50, 11568–11580

Scheme 5

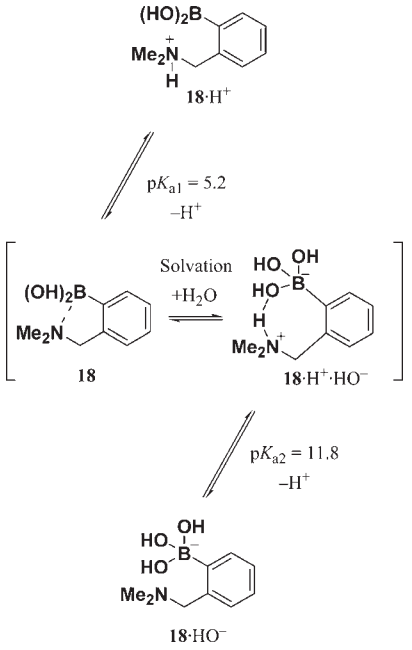

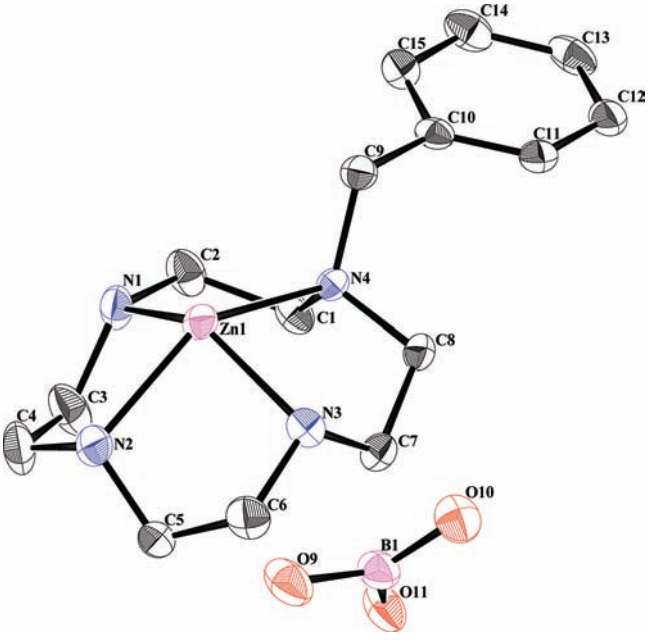

Figure 4. ORTEP drawing of **9a** and $B(OH)_3$ obtained after the reaction of **5** (L^6) with Zn^{2+} (50% probability ellipsoids). Selected bond lengths [Å]: Zn(1)−N(1) 2.130(3), Zn(1)−N(2) 2.138(3), Zn(1)−N(3) 2.100(3), Zn(1)−N(4) 2.214(3), B(1)−O(9) 1.376(5), B(1)−O(10) 1.366(5), B(1)−O(11) 1.370(5). One molecule of **9a**, four trifluoroacetate anions, two waters, and hydrogen atoms have been omitted for clarity.

Similar spectral changes were observed for Cu^{2+}, Fe^{2+}, Co^{2+}, and Ni^{2+} but not for Ca^{2+} and Mg^{2+} (Supporting Information, Figures S2−S7 and Table 2). Interestingly, the ^{11}B signal change was not observed in the case of Fe^{3+}, while the signal change was observed when Fe^{2+} was present (Supporting Information,

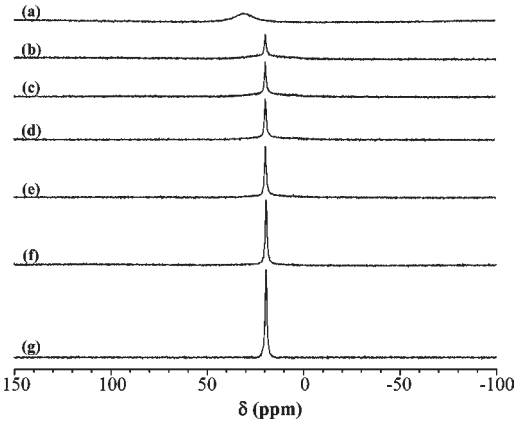

Figure 5. ^{11}B NMR (128 MHz) spectral change of **5** (L^6) (20 mM) in the presence of $ZnSO_4$ (20 mM) in D_2O at pD 7.4 (1 M HEPES buffer) and 25 °C. (a) Before the addition of Zn^{2+}. (b) 0−8 min, (c) 8−16 min, (d) 16−24 min, (e) 32−40 min, (f) 64−72 min after the addition of Zn^{2+}. (g) $B(OH)_3$ in D_2O at pD 7.4 (1 M HEPES buffer) and 25 °C. All data were referenced to external $BF_3 \cdot Et_2O$ in $CDCl_3$ (δ = 0 ppm).

Table 2. ^{11}B NMR Spectral Change of 5 (L^6) (20 mM) upon Addition of d-Block Metal Ions (20 mM) in 1 M HEPES Buffer at pD 7.4 and 25 °C[a]

	δ (ppm)	$\Delta\delta$ (ppm)[b]	time (h)[c]		δ (ppm)	$\Delta\delta$ (ppm)[b]	time (h)[c]
5 (L^6) alone	31.1			Mn^{2+}	20.6	−10.5	48
Zn^{2+}	19.4	−11.7	0.5	Ni^{2+}	19.8	−11.3	2
Cu^{2+}	19.5	−11.6	1.5	Cd^{2+}	19.2	−11.9	0.1
Fe^{2+}	19.7	−11.6	0.5	Ca^{2+}	31.7	0.6	
Fe^{3+}	30.8	−0.3		Mg^{2+}	31.9	0.8	
Co^{2+}	19.6	−11.5	1				

[a] All data were referenced to external $BF_3 \cdot Et_2O$ in $CDCl_3$ (δ = 0 ppm). [b] $\Delta\delta = \delta$ (**5** (L^6) with metal ions) − δ (**5** (L^6)). [c] Approximate reaction time for completion of C−B bond cleavage.

Figure S8 and Table 2). The results of potentiometric pH titrations of cyclen (L^1) with Fe^{2+} and Fe^{3+} (data not shown), provide proof for complexations with Fe^{2+} and Fe^{3+}. These results are consistent with our previous results, which indicated that complexation with Fe^{3+} did not facilitate the hydrolysis of sulfonate group on the side chain of $PhSO_2$-caged 8-quinolinol-pendant cyclen **23** (L^{11}) (See Scheme 6).[10c] Hydrolysis of the C−B bond with Mn^{2+} (Supporting Information, Figure S9 and Table 2) was slow, possibly because of the complexation of binuclear Mn^{3+} and Mn^{4+} produced by air oxidation.[24] The carbon−boron cleavage of **5** with Cd^{2+} was faster than that with Zn^{2+} (Supporting Information, Figure S10 and Table 2). It is likely that Cd^{2+}-bound HO^- functions as stronger nucleophile than Zn^{2+}-bound HO^-, as we previously observed.[10b,c]

For comparison, the same reaction was carried out using the meta isomer **16** (L^9), which resulted in negligible C−B bond cleavage (data not shown). Moreover, the C−B bond cleavage of phenylboronic acid (**17**) was negligible in the presence of **1** after 3 h (<5% after 1 day). These results allowed us to conclude that C−B bond cleavage of ZnL^6 complex (**7** in Scheme 2) proceeds in an intramolecular manner rather than an intermolecular manner.

dx.doi.org/10.1021/ic201507q |*Inorg. Chem.* 2011, 50, 11568–11580

Scheme 6

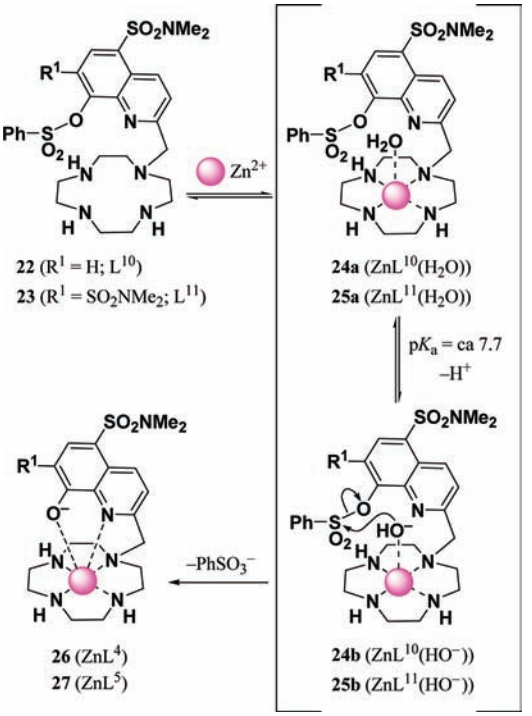

^{11}B NMR spectra of **5** (L^6) and boric acid ($B(OH)_3$) in the presence of biorelevant molecules such as sugars were investigated because it is known to interact with boronic acids and boric acid to form esters.[40] As shown in Figure S11 and S12 in the Supporting Information, D-glucose (10 mM), D-fructose (10 mM), and D-galactose (10 mM) scarcely affected the ^{11}B NMR spectra of **5** (1 mM) and boric acid (1 mM) at these concentrations. We further studied an influence of hydrogen peroxide (H_2O_2) on the ^{11}B NMR spectra of **5** (L^6). Hydrogen peroxide is one of reactive oxygen species and known to react with boronic acids and boronic acid esters especially under basic conditions.[41] As shown in Figure S13 in the Supporting Information, the broad signal of **5** (20 mM) at 31 ppm shifted to a broad signal at 5 ppm upon the addition of H_2O_2 (20 mM), implying possible interaction between the boron and H_2O_2 (Supporting Information, Figure S13b). After 12 and 24 h, partial formation of boric acid ($B(OH)_3$) was observed (~20%), indicating that careful consideration is required in the presence of H_2O_2 at this level of concentration (Supporting Information, Figures S13c and S13d). The further addition of Zn^{2+} ion to the mixture of **5** and H_2O_2 (to the solution of Supporting Information, Figure S13d) induced the hydrolysis of the C–B bond within 40 min (Supporting Information, Figure S13e).

UV Spectral Change of 5 (L^6) with Zn^{2+} and the Kinetic Study of the Carbon–Boron Bond Cleavage. To determine the kinetic parameters for the Zn^{2+}-promoted C–B bond cleavage of **5**, UV absorption measurements were carried out. The curve (a) in Figure 6 shows a UV absorption spectrum of 1 mM **5** (L^6) at pH 7.4 (100 mM HEPES) and 35 °C, which shows an absorption maximum at 268 nm ($\varepsilon = 371\ M^{-1}\cdot cm^{-1}$). Curve (b) is the UV spectrum of **5** immediately after the addition of Zn^{2+}, suggesting the formation of a Zn^{2+} complex of **5** (**7a** in Scheme 2 and Scheme 8). After that, the UV spectra changed to curve (c–e) in Figure 6, reaching the UV spectrum of

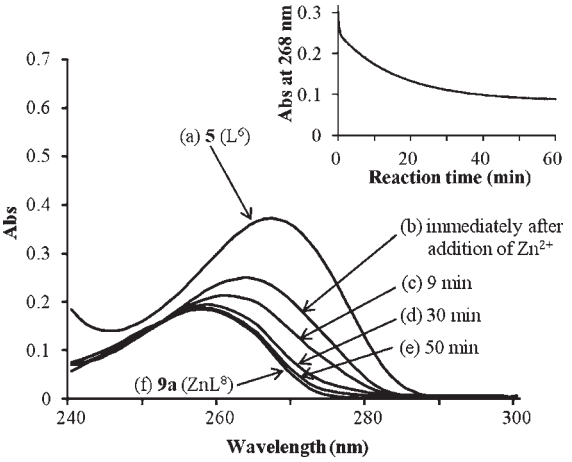

Figure 6. UV spectral change of **5** (L^6) in the presence of Zn^{2+} at pH 7.4 (100 mM HEPES) and 35 °C. (a) 1 mM **5** (L^6) in the absence of Zn^{2+}. (b) The UV spectrum was measured immediately after the addition of Zn^{2+} (1 mM) to the solution (a). Spectra after (c) 9 min, (d) 30 min, and (e) 50 min of the spectrum (b). (f) The UV spectrum of an authentic sample **9a** (1 mM) at pH 7.4 (100 mM HEPES) and 35 °C. The inset figure shows the time course for the absorption at 268 nm.

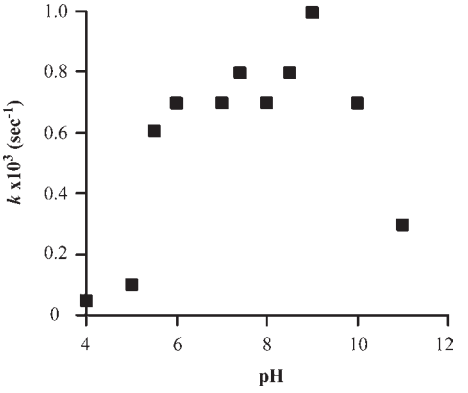

Figure 7. pH–rate constant profile for the first-order rate constants of the carbon–boron bond cleavage of 1 mM **5** (L^6) in the presence of 1 mM Zn^{2+} at 35 °C.

an authentic sample **9a** (curve (f)). Figure S14 in the Supporting Information displays the time course for the C–B bond cleavage of **5** (1.0 mM), as determined by UV absorption spectral changes upon the addition of Zn^{2+} (1.0 mM) at the pH range of 4.0–11.0 (100 mM buffer solution) and 35 °C, from which the first-order rate constants, k_1 (sec^{-1}), at pH 4.0–11.0 were determined and plotted in Figure 7. The pH–k_1 profiles indicate that the reaction rate of **5** with Zn^{2+} at neutral pH ($k_1 = 8 \times 10^{-4}\ s^{-1}$ at pH 7.4) was much greater than the corresponding reation at acidic and basic pH. It has been reported that the rate constant for the complex formation of $[Zn(OAc)]^+$ and protonated cyclen (HL^1) was $1.3 \times 10^5\ M^{-1}\cdot sec^{-1}$ in 0.1 M acetate buffer at 25 °C and the reaction was too fast to be followed with the polarographic method at pH values higher than 6.[20] Therefore, it can be assumed that the rate–determining step involves a carbon–boron bond cleavage step, as discussed in the next paragraph.

Reaction Mechanism of the C–B Bond Cleavage Reaction. The pH–k_1 profiles in Figure 7 implies two kinetic

dx.doi.org/10.1021/ic201507q |Inorg. Chem. 2011, 50, 11568–11580

Scheme 7

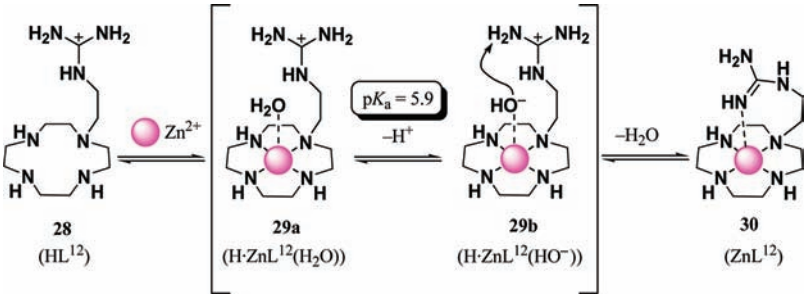

Scheme 8

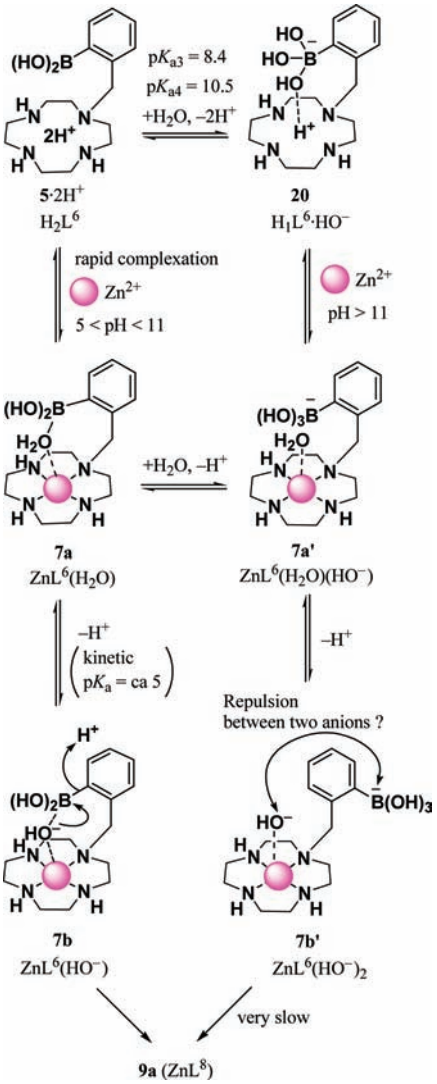

pK_a values (ca. 5 and 10−11) for **7**. For reference, Zn^{2+}-promoted hydrolysis of the sulfonate group of $PhSO_2$-caged 8-quinolinol-pendant cyclen **22** (L^{10}) and **23** (L^{11}) was previously reported.[10b,c] It was concluded that the hydrolysis is promoted by the Zn^{2+}-bound HO^- (**24b** and **25b** in Scheme 6) to give fluorescent Zn^{2+} complexes (**26** and **27**) and the kinetic pK_a values for Zn^{2+}-bound H_2O in **24** and **25** were estimated to be about 7.7.

In other work, it was reported that the pK_a value of the Zn^{2+}-bound H_2O of **29a** ($H\cdot ZnL^{12}(H_2O)$), which is a Zn^{2+} complex of the guanidine-pendant cyclen **28** (L^{12}) shown in Scheme 7, was significantly lowered as the result of the influence of the guanidinium cation (pK_a = 5.9 for **29a** ⇄ **29b**).[42] The deprotonation of the guanidinium cation by Zn^{2+}-bound HO^- (**29b**) resulted in the formation of an unusual Zn^{2+}−guanidine coordination bond (in **30**). We thus assume that the first kinetic pK_a of **7** (ca. 5) found in Figure 7 corresponds to the pK_a value for Zn^{2+}-bound H_2O in the presence of the adjacent Lewis acidic boron (for **7a** ⇄ **7b** + H^+ in Scheme 2).

From these data, a reaction mechanism for C−B bond cleavage in Zn^{2+} complex of **5** is proposed in Scheme 8, showing two possible scenarios depending on the pH of the solution. At pH > 5, cyclen part of L^6 binds to Zn^{2+} to form **7a** ($ZnL^6(H_2O)$),[8−10] in which the Zn^{2+}-bound H_2O is deprotonated to afford **7b** ($ZnL^6(HO^-)$), resulting in carbon−boron bond cleavage to yield the complex **9a** (ZnL^8). At basic condition (at pH >11), electronic repulsion between the boronate anion and Zn^{2+}-bound HO^- in **7b′**, which would be formed via **7a′**, may hamper the cleavage of the C−B bond (The formation of Zn^{2+} complex of **5** at pD 11 was confirmed by ^1H NMR experiment). Therefore, it is presumed that the second kinetic pK_a of Zn^{2+}−bound H_2O in **7** (10−11) found in Figure 7 may correspond to the equilibrium between **7a′** ⇄ **7b′**.

Uptake of 5 (L^6) and 6 (L^7) in Jurkat T Cells, and in-Cell ^{11}B NMR for Detection of Zn^{2+}. These results allowed us to conduct in-cell NMR experiments[13a,43] for the detection of intracellular Zn^{2+} using **5**. Lippard et al. reported a MRI sensor (100 μM in culture medium) for the detection of Zn^{2+} (200 μM in culture medium) introduced by using a Zn^{2+} complex of pyrithione (Zn^{2+} ionophore) into HEK-293 cells.[15d] To the best of our knowledge, this is the only report on the MRI sensor used for metal ions in cells and tissues.

Prior to the NMR measurements, the intracellular uptake of **5** (L^6) was examined utilizing Jurkat T cells (Scheme 9). The Jurkat T cells (2×10^7 cells) were incubated in 10% FCS−RPMI medium containing 33 μM **5** (L^6) and a 5% CO_2 environment at 37 °C for 1 h. After washing the cells with 0.5% CS−RPMI medium and PBS, they were lysed in RIPA buffer on ice for 30 min and analyzed by ICP−AES. Unfortunately, the amount of boron was very low in Jurkat T cells (Figure 8).

Therefore, a more cell-membrane permeable boronic acid ester **6** (L^7) was synthesized (Schemes 2 and 3). These types of boronic acid esters are known to be stable in aqueous media.[44] Indeed, the change in the ^1H NMR spectra of the **6** (L^7) in D_2O (pD 7.4) without Zn^{2+} for 12 h at 37 °C was negligible

dx.doi.org/10.1021/ic201507q |Inorg. Chem. 2011, 50, 11568–11580

Scheme 9

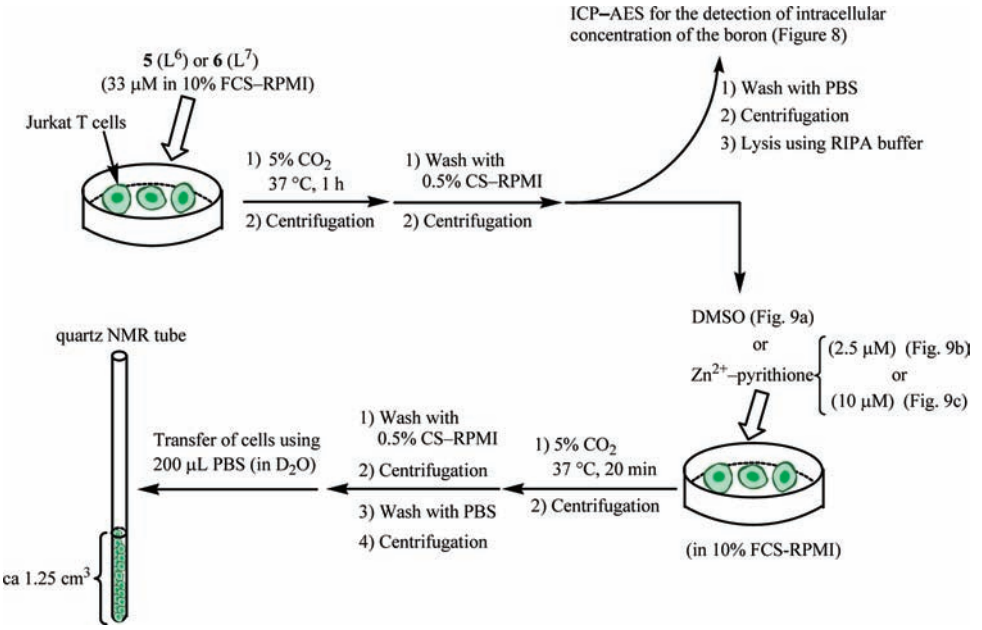

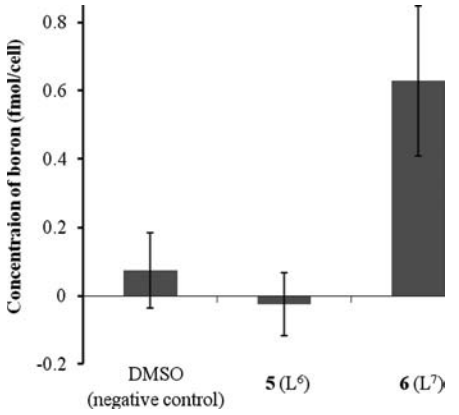

Figure 8. Concentration of **5** (L^6) and **6** (L^7) in Jurkat T cells (2×10^7 cells), determined by ICP−AES (249.733 nm) after incubation with 33 μM **5** (L^6) or 33 μM **6** (L^7) for 1 h at 37 °C and lysis using RIPA buffer. DMSO alone was used for the negative control. The error bars display standard deviation from three independent experiments.

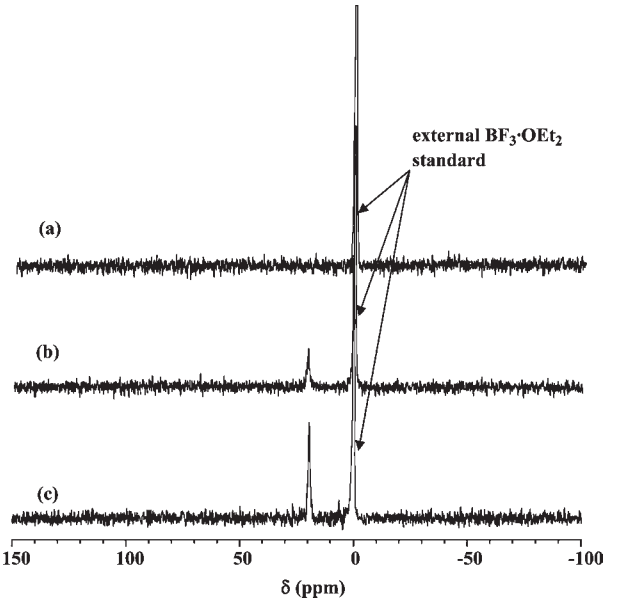

Figure 9. In-cell ^{11}B NMR spectra of **6** (L^7) in the absence of Zn^{2+}−pyrithion (ionophore), and in the presence of Zn^{2+}−pyrithion ($BF_3 \cdot Et_2O$ was used as an external references). The Jurkat T cells (4×10^8 cells) were incubated with 33 μM **6** (L^7) in culture medium at 37 °C for 1 h, and then (a) DMSO (as negative control), (b) 2.5 μM Zn^{2+}−pyrithione, and (c) 10 μM Zn^{2+}−pyrithione at 37 °C for 20 min.

(Supporting Information, Figure S15). The addition of Zn^{2+} to **6** (20 mM) induced C−B bond cleavage to give $B(OH)_3$ and slightly water-soluble diol **13**, which are formed by rapid hydrolysis of the corresponding boronic acid ester (Supporting Information, Figures S16 and S17). Moreover, a precipitate formed in this aqueous reaction mixture was isolated and identified as diol **13** by ^{1}H NMR in $CDCl_3$ (data not shown). A similar ^{11}B NMR signal change of **6** (L^7) was observed for other metal ions such as Cu^{2+}, Fe^{2+}, Co^{2+}, Ni^{2+}, and Mn^{2+} (Supporting Information, Table S1). The intracellular uptake of **6** into Jurkat T cells was improved (0.63 ± 0.22 fmol/cell), as shown in Figure 8.

We next investigated the Zn^{2+}-induced C−B bond cleavage of **6** (L^7) in Jurkat T cells (bottom half of Scheme 9). Jurkat T cells (4×10^8 cells) were incubated with **6** (final concentration 33 μM) under the same condition as those with **5**, washed with 0.5% CS−RPMI, and incubated with either 2.5 or 10 μM Zn^{2+}−pyrithione, or DMSO (as a negative control) at 37 °C for 20 min. The cells were sequentially washed with 0.5% CS−RPMI and PBS, and transferred to a quartz NMR tube containing external $BF_3 \cdot Et_2O$ standard using 200 μL of PBS prepared in D_2O (estimated volume of whole cells = ca. 1.25 cm^3). ^{11}B NMR spectra were recorded and compared for cell pellets with and without exogenously introduced Zn^{2+}.

dx.doi.org/10.1021/ic201507q |*Inorg. Chem.* 2011, 50, 11568–11580

As shown in Figure 9a, the signal of **6** at about 31 ppm in the absence of Zn^{2+} is too broad to be observed at this concentration in the ^{11}B NMR. In contrast, the signal at 19 ppm that corresponds to $B(OH)_3$ was observed in response to the concentration of Zn^{2+} (Figure 9b and 9c).[45,46]

CONCLUSION

We describe the sensing of biologically essential d-block metal cations such as Zn^{2+}, Cu^{2+}, Fe^{2+}, Co^{2+}, Ni^{2+}, and Mn^{2+} based on the ^{11}B NMR signals of **5** (L^6) and **6** (L^7) in aqueous solution at physiological pH. The carbon−boron bonds of simple ^{11}B NMR probes, **5** and **6**, were cleaved upon the addition of d-block metal ions and the broad ^{11}B NMR signal at 31 ppm was shifted to a sharp signal at 19 ppm, which corresponds to $B(OH)_3$, as confirmed by ^1H NMR, X-ray single crystal structure analysis, and UV absorption spectra. In addition, more cell-membrane permeable boronic acid ester **6** was used for the ^{11}B NMR sensing of Zn^{2+} in Jurkat T cells. The signal corresponding to $B(OH)_3$ was observed in response to the concentration of Zn^{2+} in Jurkat T cells, while such a signal was not observed in the absence of Zn^{2+}.[47] These results suggest that the ^{11}B NMR sensing of Zn^{2+} and other d-block metal ions by **6** (L^7) and its derivatives may afford a potential "chemical shift imaging (CSI)"[13a,48] technique in the biomedical sciences.

It has been suggested that decrease of the Zn^{2+} and other metal ions are potent candidates as biomarkers for diagnosis of prostate and other cancers.[5] Moreover, it is suggested that ^{11}B and ^{10}B NMR is useful for the detection of ^{10}B-containing agents such as carborane and L-4-boronophenylalanine in the boron neutron capture therapy (BNCT).[26c,d,f] Our results may provide a basic concept to suggest that ^{11}B NMR sensing of Zn^{2+} and other d-block metal ions based on chemical reaction of boron is useful for a diagnosis and treatment of cancers and other diseases in combination with BNCT and other medical technologies.

ASSOCIATED CONTENT

Supporting Information. ^1H NMR, ^{13}C NMR, and ^{11}B NMR of **5** (L^6) and **6** (L^7). Deprotonation behavior of **16** (L^9) in Scheme S1. Figures S1−S14. Table S1 for the C−B bond cleavage of **6** (L^7) with d-block metal ions. Tables and CIF for the X-ray crystal structure analysis of **5** (H_2L^6) and **9a**. This material is available free of charge via the Internet at http://pubs.acs.org.

AUTHOR INFORMATION

Corresponding Author
*E-mail: shinaoki@rs.noda.tus.ac.jp.

ACKNOWLEDGMENT

This work was supported by grants-in-aid from the Ministry of Education, Culture, Sports, Science and Technology (MEXT) of Japan (Nos. 19659026, 22390005, and 22659055 for S.A. and No. 20750081 for M.K.) and "Academic Frontier" project for private universities: matching fund subsidy from MEXT, 2009−2013. M.K. is thankful for Sasakawa Grants for Science Fellows (SGSF) from the Japan Science Society.

REFERENCES

(1) (a) Mertz, W. *Science* **1981**, *213*, 1332–1338. (b) Maret, W. *BioMetals* **2001**, *14*, 187–190. (c) Finney, L. A.; O'Halloran, T. V. *Science* **2003**, *300*, 931–936.

(2) (a) Palmer, A. E.; Franz, K. J. *Chem. Rev.* **2009**, *109*, 4533–4535. (b) Maret, W.; Li, Y. *Chem. Rev.* **2009**, *109*, 4682–4707.

(3) (a) O'Halloran, T. V.; Culotta, V. C. *J. Biol. Chem.* **2000**, *275*, 25057–25060. (b) Outten, C. E.; O'Halloran, T. V. *Science* **2001**, *292*, 2488–2492. (c) Outten, C. E.; Tobin, D. A.; Penner-Hahn, J. E.; O'Halloran, T. V. *Biochemistry* **2001**, *40*, 10417–10423. (d) Arnesano, F.; Banci, L.; Bertini, I.; Ciofi-Baffoni, S. *Eur. J. Inorg. Chem.* **2004**, 1583–1593. (e) Sekhon, B. S. *Curr. Chem. Biol.* **2008**, *4*, 173–186. (f) Ma, Z.; Jacobsen, F. E.; Giedroc, D. P. *Chem. Rev.* **2009**, *109*, 4644–4681. (g) Waldron, K. J.; Rutherford, J. C.; Ford, D.; Robinson, N. J. *Nature* **2009**, *460*, 823–830.

(4) (a) Cuajungco, M. P.; Lees, G. J. *Neurobiol. Dis.* **1997**, *4*, 137–169. (b) Waggoner, D. J.; Bartnikas, T. B.; Gitlin, J. D. *Neurobiol. Dis.* **1999**, *6*, 221–230. (c) Bush, A. I.; Tanzi, R. E. *Proc. Natl. Acad. Sci. U. S. A.* **2002**, *99*, 7317–7319. (d) Valentine, J. S.; Hart, P. J. *Proc. Natl. Acad. Sci. U. S. A.* **2003**, *100*, 3617–3622. (e) Hambidge, K. M.; Krebs, N. F. *J. Nutr.* **2007**, *137*, 1101–1105. (f) Stewart-Knox, B. J.; Simpson, E. E. A.; Parr, H.; Rae, G.; Polito, A.; Intorre, F.; Sanchez, M. A.; Meunier, N.; O'Connor, J. M.; Maiani, G.; Coudray, C.; Strain, J. J. *Br. J. Nutr.* **2008**, *99*, 129–136.

(5) (a) Ghosh, S. K.; Kim, P.; Zhang, X.; Yun, S.-H.; Moore, A.; Lippard, S. J.; Medarova, Z. *Cancer Res.* **2010**, *70*, 6119–6127. (b) Costello, L. C.; Franklin, R. B. *Prostate Cancer Prostatic Dis.* **2008**, 1–8. (c) Franklin, R. B.; Costello, L. C. *Archiv. Biochem. Biophys.* **2007**, *463*, 211–217. (d) Costello, L. C.; Franklin, R. B. *Mol. Cancer* **2006**, *5*, 17. (e) Shilstein, S. S.; Cortesi, M.; Breskin, A.; Chechik, R.; Vartsky, D.; Raviv, G.; Kleinman, N.; Ramon, J.; Kogan, G.; Gladysh, V.; Moriel, E.; Huszar, M.; Volkov, A.; Fridman, E. *Talanta* **2006**, *70*, 914–921.

(6) See reviews on fluorescent sensors of zinc and other d-block metal ions: (a) Kimura, E.; Koike, T. *Chem. Soc. Rev.* **1998**, *27*, 179–184. (b) Prodi, L.; Bolletta, F.; Montalti, M.; Zaccheroni, N. *Coord. Chem. Rev.* **2000**, *205*, 59–83. (c) Kimura, E.; Aoki, S. *BioMetals* **2001**, *14*, 191–204. (d) Jiang, P.; Guo, Z. *Coord. Chem. Rev.* **2004**, *248*, 205–229. (e) Kikuchi, K.; Komatsu, K.; Nagano, T. *Curr. Opin. Chem. Biol.* **2004**, *8*, 182–191. (f) Lim, N. C.; Freake, H. C.; Brückner, C. *Chem.—Eur. J.* **2005**, *11*, 38–49. (g) Dai, Z.; Canary, J. W. *New J. Chem.* **2007**, *31*, 1708–1718. (h) Carol, P.; Sreejith, S.; Ajayaghosh, A. *Chem.—Asian. J.* **2007**, *2*, 338–348. (i) Que, E. L.; Domaille, D. W.; Chang, C. J. *Chem. Rev.* **2008**, *108*, 1517–1549. (j) Nolan, E. M.; Lippard., S. J. *Acc. Chem. Res.* **2009**, *42*, 193–203. (k) Xu, Z.; Yoon, J.; Spring, D. R. *Chem. Soc. Rev.* **2010**, *39*, 1996–2006.

(7) See selected recent papers on fluorescent sensors of zinc and other d-block metal ions: (a) Sumalekshmy, S.; Henary, M. M.; Siegel, N.; Lawson, P. V.; Wu, Y.; Schmidt, K.; Brédas, J.-L.; Perry, J. W.; Fahrni, C. J. *J. Am. Chem. Soc.* **2007**, *129*, 11888–11889. (b) Ke, Q.; Davidson, T.; Kluz, T.; Oller, A.; Costa, M. *Toxicol. Appl. Pharmacol.* **2007**, *219*, 18–23. (c) Zhang, X.; Hayes, D.; Smith, S. J.; Friedle, S.; Lippard, S. J. *J. Am. Chem. Soc.* **2008**, *130*, 15788–15789. (d) Zhang, L.; Murphy, C. S.; Kuang, G.-C.; Hazelwood, K. L.; Constantino, M. H.; Davidson, M. W.; Zhu, L. *Chem. Commun.* **2009**, 7408–7410. (e) Qian, F.; Zhang, C.; Zhang, Y.; He, W.; Gao, X.; Hu, P.; Guo, Z. *J. Am. Chem. Soc.* **2009**, *131*, 1460–1468. (f) Wong, B. A.; Friedle, S.; Lippard, S. J. *J. Am. Chem. Soc.* **2009**, *131*, 7142–7152. (g) Ambrosi, G.; Formica, M.; Fusi, V.; Giorgi, L.; Macedi, E.; Micheloni, M.; Paoli, P.; Pontellini, R.; Rossi, P. *Inorg. Chem.* **2010**, *49*, 9940–9948. (h) Xu, Y.; Meng, J.; Meng, L.; Dong, Y.; Cheng, Y.; Zhu, C. *Chem.—Eur. J.* **2010**, *16*, 12898–12903. (i) Pathak, R. K.; Dikundwar, A. G.; Row, T. N. G.; Rao, C. P. *Chem. Commun.* **2010**, *46*, 4345–4347. (j) Xu, Z.; Baek, K.-H.; Kim, H. N.; Cui, J.; Qian, X.; Spring, D. R.; Shin, I.; Yoon, J. *J. Am. Chem. Soc.* **2010**, *132*, 601–610. (k) Chaudhry, A. F.; Verma, M.; Morgan, M. T.; Henary, M. M.; Siegel, N.; Hales, J. M.; Perry, J. W.; Fahrni, C. J. *J. Am. Chem. Soc.* **2010**, *132*, 737–747. (l) Lee, D. Y.; Singh, N.; Jang, D. O. *Tetrahedron Lett.*

2010, *51*, 1103–1106. (m) Saha, U. C.; Chattopadhyay, B.; Dhara, K.; Mandal, S. K.; Sarkar, S.; Khuda-Bukhsh, A. R.; Mukherjee, M.; Helliwell, M.; Chattopadhyay, P. *Inorg. Chem.* **2011**, *50*, 1213–1219. (n) Chaudhry, A. F.; Mandal, S.; Hardcastle, K. I.; Fahrni, C. J. *Chem. Sci.* **2011**, *2*, 1016–1024. (o) Buccella, D.; Horowitz, J. A.; Lippard, S. J. *J. Am. Chem. Soc.* **2011**, *133*, 4101–4114.

(8) (a) Koike, T.; Watanabe, T.; Aoki, S.; Kimura, E.; Shiro, M. *J. Am. Chem. Soc.* **1996**, *118*, 12696–12703. (b) Kimura, E.; Aoki, S.; Kikuta, E.; Koike, T. *Proc. Natl. Acad. Sci. U. S. A.* **2003**, *100*, 3731–3736. (c) Kimura, E.; Takasawa, R.; Tanuma, S.; Aoki, S. *Science STKE* **2004**, *223*, 7.

(9) Aoki, S.; Kagata, D.; Shiro, M.; Takeda, K.; Kimura, E. *J. Am. Chem. Soc.* **2004**, *126*, 13377–13390.

(10) (a) Aoki, S.; Sakurama, K.; Matsuo, N.; Yamada, Y.; Takasawa, R.; Tanuma, S.; Shiro, M.; Takeda, K.; Kimura, E. *Chem.—Eur. J.* **2006**, *12*, 9066–9080. (b) Aoki, S.; Sakurama, K.; Ohshima, R.; Matsuo, N.; Yamada, Y.; Takasawa, R.; Tanuma, S.; Takeda, K.; Kimura, E. *Inorg. Chem.* **2008**, *47*, 2747–2754. (c) Ohshima, R.; Kitamura, M.; Morita, A.; Shiro, M.; Yamada, Y.; Ikekita, M.; Kimura, E.; Aoki, S. *Inorg. Chem.* **2010**, *49*, 888–899.

(11) (a) Yang, L.; McRae, R.; Henary, M. M.; Patel, R.; Lai, B.; Vogt, S.; Fahrni, C. J. *Proc. Natl. Acad. Sci. U. S. A.* **2005**, *102*, 11179–11184. (b) Zeng, L.; Miller, E. W.; Pralle, A.; Isacoff, E. Y.; Chang, C. J. *J. Am. Chem. Soc.* **2006**, *128*, 10–11. (c) Domaille, D. W.; Zeng, L.; Chang, C. J. *J. Am. Chem. Soc.* **2010**, *132*, 1194–1195. (d) Wegner, S. V.; Arslan, H.; Sunbul, M.; Yin, J.; He, C. *J. Am. Chem. Soc.* **2010**, *132*, 2567–2569.

(12) (a) Rurack, K.; Kollmannsberger, M.; Resch-Genger, U.; Daub, J. *J. Am. Chem. Soc.* **2000**, *122*, 968–969. (b) Rapisarda, V. A.; Volentini, S. I.; Farías, R. N.; Massa, E. M. *Anal. Biochem.* **2002**, *307*, 105–109. (c) Liu, J.-M.; Zheng, Q.-Y.; Yang, J.-L.; Chen, C.-F.; Huang, Z.-T. *Tetrahedron Lett.* **2002**, *43*, 9209–9212. (d) Ma, Y.; Luo, W.; Camplo, M.; Liu, Z.; Hider, R. C. *Bioorg. Med. Chem. Lett.* **2005**, *15*, 3450–3452. (e) Huang, X.; Dong, Y.; Meng, J.; Cheng, Y.; Zhu, C. *Synlett* **2010**, 1841–1844. (f) Tan, S. S.; Kim, S. J.; Kool, E. T. *J. Am. Chem. Soc.* **2011**, *133*, 2664–2671.

(13) (a) de Graaf, R. A. *in vivo NMR Spectroscopy Principles and Techniques*, 2nd ed.; John Wiley and Sons: Chichester, 2007. (b) Caravan, P.; Ellison, J. J.; McMurry, T. J.; Lauffer, R. B. *Chem. Rev.* **1999**, *99*, 2293–2352. (c) Werner, E. J.; Datta, A.; Jocher, C. J.; Raymond, K. N. *Angew. Chem., Int. Ed.* **2008**, *47*, 8568–8580. (d) Jennings, L. E.; Long, N. J. *Chem. Commun.* **2009**, 3511–3524.

(14) Reviews: (a) McRae, R.; Bagchi, P.; Sumalekshmy, S.; Fahrni, C. J. *Chem. Rev.* **2009**, *109*, 4780–4827. (b) Haas, K. L.; Franz, K. J. *Chem. Rev.* **2009**, *109*, 4921–4960. (c) Bonnet, C. S.; Tóth, É. *Future Med. Chem.* **2010**, *2*, 367–384. (d) Que, E. L.; Chang, C. J. *Chem. Soc. Rev.* **2010**, *39*, 51–60.

(15) (a) Hanaoka, K.; Kikuchi, K.; Urano, Y.; Nagano, T. *J. Chem. Soc., Perkin Trans. 2* **2001**, 1840–1843. (b) Hanaoka, K.; Kikuchi, K.; Urano, Y.; Narazaki, M.; Yokawa, T.; Sakamoto, S.; Yamaguchi, K.; Nagano, T. *Chem. Biol.* **2002**, *9*, 1027–1032. (c) Trokowski, R.; Ren, J.; Kálmán, F. K.; Sherry, A. D. *Angew. Chem., Int. Ed.* **2005**, *44*, 6920–6923. (d) Zhang, X.; Lovejoy, K. S.; Jasanoff, A.; Lippard, S. J. *Proc. Natl. Acad. Sci. U. S. A.* **2007**, *104*, 10780–10785. (e) Major, J. L.; Parigi, G.; Luchinat, C.; Meade, T. J. *Proc. Natl. Acad. Sci. U. S. A.* **2007**, *104*, 13881–13886. (f) Major, J. L.; Boiteau, R. M.; Meade, T. J. *Inorg. Chem.* **2008**, *47*, 10788–10795. (g) Esqueda, A. C.; López, J. A.; Andreu-de-Riquer, G.; Alvarado-Monzón, J. C.; Ratnakar, J.; Lubag, A. J. M.; Sherry, A. D.; León-Rodríguez, L. M. D. *J. Am. Chem. Soc.* **2009**, *131*, 11387–11391. (h) You, Y.; Tomad, E.; Hwang, K.; Atanasijevic, T.; Nam, W.; Jasanoff, A. P.; Lippard, S. J. *Chem. Commun.* **2010**, *46*, 4139–4141.

(16) (a) Que, E. L.; Chang, C. J. *J. Am. Chem. Soc.* **2006**, *128*, 15942–15943. (b) Que, E. L.; Gianolio, E.; Baker, S. L.; Wong, A. P.; Aime, S.; Chang, C. J. *J. Am. Chem. Soc.* **2009**, *131*, 8527–8536.

(17) (a) Ruloff, R.; van Koten, G.; Merbach, A. E. *Chem. Commun.* **2004**, 842–843. (b) Livramento, J. B.; Tóth, É.; Sour, A.; Borel, A.; Merbach, A. E.; Ruloff, R. *Angew. Chem., Int. Ed.* **2005**, *44*, 1480–1484. (c) Paris, J.; Gameiro, C.; Humblet, V.; Mohapatra, P. K.; Jacques, V.; Desreux, J. F. *Inorg. Chem.* **2006**, *45*, 5092–5102.

(18) (a) Li, W.; Fraser, S. E.; Meade, T. J. *J. Am. Chem. Soc.* **1999**, *121*, 1413–1414. (b) Li, W.; Parigi, G.; Fragai, M.; Luchinat, C.; Meade, T. J. *Inorg. Chem.* **2002**, *41*, 4018–4024. (c) Atanasijevic, T.; Shusteff, M.; Fam, P.; Jasanoff, A. *Proc. Natl. Acad. Sci. U. S. A.* **2006**, *103*, 14707–14712. (d) Angelovski, G.; Fouskova, P.; Mamedov, I.; Canals, S.; Toth, E.; Logothetis, N. K. *ChemBioChem* **2008**, *9*, 1729–1734. (e) Dhingra, K.; Maier, M. E.; Beyerlein, M.; Angelovski, G.; Logothetis, N. K. *Chem. Commun.* **2008**, 3444–3446. (f) Dhingra, K.; Fousková, P.; Angelovski, G.; Maier, M. E.; Logothetis, N. K.; Tóth, É. *J. Biol. Inorg. Chem.* **2008**, *13*, 35–46. (g) Mishra, A.; Fousková, P.; Angelovski, G.; Balogh, E.; Mishra, A. K.; Logothetis, N. K.; Tóth, É. *Inorg. Chem.* **2008**, *47*, 1370–1381. (h) Khatua, S.; Choi, S. H.; Lee, J.; Huh, J. O.; Do, Y.; Churchill, D. G. *Inorg. Chem.* **2009**, *48*, 1799–1801. (i) Atanasijevic, T.; Zhang, X.; Lippard, S. J.; Jasanoff, A. *Inorg. Chem.* **2010**, *49*, 2589–2591.

(19) MRI probe for Ca^{2+}, K^{+}, Mg^{2+}: Hifumi, H.; Tanimoto, A.; Citterio, D.; Komatsu, H.; Suzuki, K. *Analyst* **2007**, *132*, 1153–1160.

(20) For Zn^{2+} :Kodama, M.; Kimura, E. *J. Chem. Soc., Dalton Trans.* **1977**, 2269–2276.

(21) For Cu^{2+}: (a) Kodama, M.; Kimura, E. *J. Chem. Soc., Chem. Commun.* **1975**, 326–327. (b) Kodama, M.; Kimura, E. *J. Chem. Soc., Dalton Trans.* **1976**, 116–120.

(22) For Co^{3+}: (a) Collman, J. P.; Schneider, P. W. *Inorg. Chem.* **1966**, *5*, 1380–1384. (b) Clarkson, A. J.; Buckingham, D. A.; Rogers, A. J.; Blackman, A. G.; Clark, C. R. *Inorg. Chem.* **2000**, *39*, 4769–4775. (c) Rawlings, J.; Cleland, W. W.; Hengge, A. C. *J. Am. Chem. Soc.* **2006**, *128*, 17120–17125. (d) Chang, J. Y.-C.; Stevenson, R. J.; Lu, G.-L.; Brothers, P. J.; Clark, G. R.; Denny, W. A.; Ware, D. C. *Dalton Trans.* **2010**, *39*, 11535–11550.

(23) For Ni^{2+}: (a) Fabbrizzi, L. *Inorg. Chem.* **1977**, *16*, 2667–2668. (b) Plassman, W. H.; Swisher, R. G.; Blinn, E. L. *Inorg. Chem.* **1980**, *19*, 1103–1104.

(24) For Mn^{3+} and Mn^{4+}: (a) Brewer, K. J.; Liegeois, A.; Otvos, J. W.; Calvin, M.; Spreer, L. O. *J. Chem. Soc., Chem. Commun.* **1988**, 1219–1220. (b) Goodson, P. A.; Hodgson, D. J. *Inorg. Chim. Acta* **1992**, *197*, 141–147. (c) Panja, A.; Shaikh, N.; Banerjee, P.; Saha, B. *Int. J. Chem. Kinet.* **2004**, *36*, 119–128.

(25) (a) Park, M.; Li, Q.; Shcheynikov, N.; Muallem, S.; Zeng, W. *Cell Cycle* **2005**, *4*, 24–26. (b) Bendel, P. *NMR Biomed.* **2005**, *18*, 74–82. (c) Ronconi, L.; Sadler, P. J. *Coord. Chem. Rev.* **2008**, *252*, 2239–2277.

(26) For reference of ^{11}B MRI: (a) Bendel, P.; Davis, M.; Berman, E.; Kabalka, G. W. *J. Magn. Reson.* **1990**, *88*, 369–375. (b) Heřmánek, S. *Chem. Rev.* **1992**, *92*, 325–362. (c) Morin, C. *Tetrahedron* **1994**, *50*, 12521–12569. (d) Kabalka, G. W.; Tang, C.; Bendel, P. *J. Neuro-Oncology* **1997**, *33*, 153–161. (e) Meder, R.; Franich, R. A.; Callaghan, P. T. *Solid State Nucl. Magn. Reson.* **1999**, *15*, 69–72. (f) Valliant, J. F.; Guenther, K. J.; King, A. S.; Morel, P.; Schaffer, P.; Sogbein, O. O.; Stephenson, K. A. *Coord. Chem. Rev.* **2002**, *232*, 173–230.

(27) Kimura, E.; Aoki, S.; Koike, T.; Shiro, M. *J. Am. Chem. Soc.* **1997**, *119*, 3068–3076.

(28) (a) Takeuchi, M.; Mizuno, T.; Shinmori, H.; Nakashima, M.; Shinkai, S. *Tetrahedron* **1996**, *52*, 1195–1204. (b) Fedorov, A. Y.; Carrara, F.; Finet, J.-P. *Tetrahedron Lett.* **2001**, *42*, 5875–5877.

(29) (a) Corey, E. J.; Danheiser, R. L.; Chadrasekaran, S. *J. Org. Chem.* **1976**, *41*, 260–265. (b) Rao, S. A.; Periasamy, M. *Tetrahedron Lett.* **1988**, *29*, 1583–1586.

(30) Cappuccio, F. E.; Suri, J. T.; Cordes, D. B.; Wessling, R. A.; Singaram, B. *J. Fluoresc.* **2004**, *14*, 521–533.

(31) Aoki, S.; Sugimura, C.; Kimura, E. *J. Am. Chem. Soc.* **1998**, *120*, 10094–10102.

(32) Martell, A. E.; Motekaitis, R. J. *Determination and Use of Stability Constants*, 2nd ed.; VCH: New York, 1992.

(33) Robinson, M. A. *J. Inorg. Nucl. Chem.* **1964**, *26*, 1277–1281.

(34) (a) Hall, D. G. In *Boronic Acids: Preparation, Applications in Organic Synthesis and Medicine*; Hall, D. G., Ed.; Wiley-VCH: Weinheim, 2005; p 10. (b) Westmark, P. R.; Gardiner, S. J.; Smith, B. D. *J. Am. Chem. Soc.* **1996**, *118*, 11093–11100.

(35) Wulff, G. *Pure Appl. Chem.* **1982**, *54*, 2093–2102.
(36) Zhu, L.; Shabbir, S. H.; Gray, M.; Lynch, V. M.; Sorey, S.; Anslyn, E. V. *J. Am. Chem. Soc.* **2006**, *128*, 1222–1232.
(37) For boronic acids having amino side chains: (a) Wiskur, S. L.; Lavigne, J. J.; Sit-Haddou, H.; Lynch, V.; Chiu, Y. H.; Canary, J. W.; Anslyn, E. V. *Org. Lett.* **2001**, *3*, 1311–1314. (b) Norrild, J. C. *J. Chem. Soc., Perkin Trans. 2* **2001**, 719–726. (c) James, T. D.; Sandanayake, S.; Iguchi, R.; Shinkai, S. *J. Am. Chem. Soc.* **1995**, *117*, 8982–8987. (d) Nishiyabu, R.; Kubo, Y.; James, T. D.; Fossey, J. S. *Chem. Commun.* **2011**, *47*, 1106–1123.
(38) For boronic acids and boronic acid esters: (a) Otsuka, H.; Uchimura, E.; Koshino, H.; Okano, T.; Kataoka, K. *J. Am. Chem. Soc.* **2003**, *125*, 3943–3502. (b) Wülff, G.; Lauer, M.; Böhnke, H. *Angew. Chem., Int. Ed. Engl.* **1984**, *23*, 741–742. (c) Burgemeister, T.; Grobe-Einsler, R.; Grotstollen, R.; Mannschreck, A.; Wulff, G. *Chem. Ber.* **1981**, *114*, 3403–3411. (d) Singhal, R. P.; Ramamurthy, B.; Govindraj, N.; Sarwar, Y. *J. Chromatogr.* **1991**, *543*, 17–38. (e) Nagai, Y.; Kobayashi, K.; Toi, H.; Aoyama, Y. *Bull. Chem. Soc. Jpn.* **1993**, *66*, 2965–2971.
(39) The ^{11}B NMR signals of **5** were too broad to determine longitudinal and transverse relaxation times (T1 and T2) of these signals.
(40) (a) James, T. D. In *Boronic Acids: Preparation, Applications in Organic Synthesis and Medicine*; Hall, D. G., Ed.; Wiley-VCH: Weinheim, 2005; pp 441−479. (b) Lorand, J. P.; Edwards, J. O. *J. Org. Chem.* **1959**, *24*, 769–774.
(41) (a) Albers, A. E.; Okreglak, V. S.; Chang, C. J. *J. Am. Chem. Soc.* **2006**, *128*, 9640–9641. (b) Miller, E. W.; Albers, A. E.; Pralle, A.; Isacoff, E. Y.; Chang, C. J. *J. Am. Chem. Soc.* **2005**, *127*, 16652–16659. (c) Lippert, A. R.; Bittner, G. C. V. D.; Chang, C. J. *Acc. Chem. Res.* **2011**, *44*, 793–804.
(42) Aoki, S.; Iwaida, K.; Hanamoto, N.; Shiro, M.; Kimura, E. *J. Am. Chem. Soc.* **2002**, *124*, 5256–5257.
(43) For in-cell NMR, see: (a) Gallice, P.; Monti, J. P.; Baz, M.; Murisasco, A.; Crevat, A. *Clin. Chem.* **1988**, *34*, 2044–2047. (b) Inomata, K.; Ohno, A.; Tochio, H.; Isogai, S.; Tenno, T.; Nakase, I.; Takeuchi, T.; Futaki, S.; Ito, Y.; Hiroaki, H.; Shirakawa, M. *Nature* **2009**, *458*, 106–110. (c) Takaoka, Y.; Sakamoto, T.; Tsukiji, S.; Narazaki, M.; Matsuda, T.; Tochio, H.; Shirakawa, M.; Hamachi, I. *Nat. Chem.* **2009**, *1*, 557–561. (d) Takaoka, Y.; Sun, Y.; Tsukiji, S.; Hamachi, I. *Chem. Sci.* **2011**, *2*, 511–520. (e) Mizukami, S.; Matsushita, H.; Takikawa, R.; Sugihara, F.; Shirakawa, M.; Kikuchi, K. *Chem. Sci.* **2011**, *2*, 1151–1155.
(44) Bernardini, R.; Oliva, A.; Paganelli, A.; Menta, E.; Grugni, M.; Munari, S. D.; Goldoni, L. *Chem. Lett.* **2009**, *38*, 750–751.
(45) The intracellular amounts of the boron in Jurkat T cells used for in-cell NMR experiments were reconfirmed by ICP−AES to be 0.64 ± 0.12 fmol/cell, which coincides with the amount of the boron reported in Figure 8. From these data, the concentration of the boron in the whole collected cell volume (ca. 1.25 cm^3) was calculated to be 0.20 ± 0.04 mM. These results also indicate that intracellular uptake of **6** is negligibly affected by the Zn^{2+} concentrations (0, 2.5, and 10 μM) in the culture medium.
(46) The working curve for the determination of the concentration of $B(OH)_3$ in the cells after the addition of Zn^{2+} was prepared using an external $BF_3 \cdot Et_2O$ in $CDCl_3$. Using their curve, the concentrations of $B(OH)_3$ in Jurkat T cells were determined to be 0.11 mM and 0.27 mM for Figure 9b and 9c, which are slightly lower than the Zn^{2+} contents in cells estimated by ICP−AES (0.62 fmol/cell (0.20 mM) for Figure 9b and 3.3 fmol/cell (1.0 mM) for Figure 9c). We assume that the Zn^{2+} added from outside of cells does not fully react with L^7, possibly because of some interactions of free Zn^{2+} with intracellular organelles or cell membranes.
(47) In our preliminary experiments, phenylboronic acid having iminodiacetate side chain instead of cyclen also undergoes C−B bond hydrolysis upon complexation with Zn^{2+}, Fe^{2+}, and Cu^{2+}. Details will be reported somewhere else.
(48) (a) Nelson, S. J.; Vigneron, D. B.; Star-Lack, J.; Kurhanewicz, J. *NMR Biomed.* **1997**, *10*, 411–422. (b) Lee, H.; Tikunov, A.; Stoskopf, M. K.; Macdonald, J. M. *Mar. Drugs* **2010**, *8*, 2369–2383. (c) Östlund, Å.; Bernin, D.; Nordstierna, L.; Nydén, M. *J. Colloid Interface Sci.* **2010**, *344*, 238–240.